Université du Québec
à Rimouski

PRÉDICTION DES ATTRIBUTS GÉOMÉTRIQUES DU JOINT DE SOUDURE DANS LE CAS DE SOUDAGE AU LASER PAR RECOUVREMENT DE TÔLES EN ACIER GALVANISÉ – MODÈLE 3D ET RESEAUX DE NEURONES

Mémoire présenté

Dans le cadre du programme de maîtrise en ingénierie.

En vue de l'obtention du grade de maître ès sciences appliquées (M.Sc.A.)

PAR

© KAMEL OUSSAID

Mai 2020

Composition du jury :

Adrian Ilinca, président du jury, Université du Québec à Rimouski

Abderrazak El Ouafi, directeur de recherche, Université du Québec à Rimouski

Ahmed Chebak, codirecteur de recherche, Université du Québec à Rimouski

Souheil-Antoine Tahan, examinateur externe, École de Technologie Supérieure

Dépôt initial le 22 Mars 2020 Dépôt final le 07 Mai 2020

A toute ma famille

REMERCIEMENTS

Je rends un grand hommage à M. Abderrazak El Ouafi pour son encadrement, son soutien et ses conseils judicieux, ainsi que pour sa disponibilité et le temps qu'il a consacré à la correction de mon travail. Je remercie également M. Ahmed Chebak pour sa contribution au premier article.

Je tiens également à remercier mes parents, mon épouse, mes frères et leurs épouses, ma sœur et son mari, mes neveux, mes amis et tous ceux qui ont contribué de près ou de loin à la réussite de ce projet de recherche.

RÉSUMÉ

Le soudage au laser est une des techniques d'assemblage qui a révolutionné de nombreux secteurs industriels, y compris le secteur de l'industrie automobile, grâce à sa productivité et à sa flexibilité. En raison de la nature focalisée du faisceau laser et de sa puissance élevée, le soudage au laser se distingue des autres procédés conventionnels par un apport de chaleur, bref et localisé, favorisant la production de soudures étroites profondes et esthétiques avec des vitesses d'exécution pouvant atteindre plusieurs cm/s, une zone affectée par la chaleur très étroite et des distorsions thermiques limitées. Pour faire face aux contraintes de positionnement précis imposé dans le cas de soudage bout à bout et de soudage d'angle, la configuration de soudage par recouvrement s'avère être mieux adaptée pour la fabrication en grande séries. Cependant, le soudage par recouvrement des aciers galvanisés peut être instable et à cause de l'évaporation prématurée du recouvrement du zinc à l'interface des tôles superposées. Des précautions additionnelles sont nécessaires pour mettre en œuvre ce procédé de façon adéquate. Le choix d'un écart optimal entre les tôles à souder combiné à une sélection adéquate des paramètres du laser peuvent résoudre le problème de l'évaporation du zinc et produire des soudures de très grande qualité.

Les propriétés mécaniques d'une soudure réalisée au laser découlent généralement de la forme et des dimensions de sa section transversale, qui dépendent elles-mêmes des paramètres du laser et des conditions de soudage telles que la puissance du laser, la vitesse d'avance du faisceau laser, le diamètre focal et l'écart entre les tôles. Pour exploiter efficacement les avantages du procédé, il faut développer une stratégie qui permet de contrôler les paramètres et les conditions de soudage pour obtenir des soudures avec les caractéristiques désirées, sans avoir recours à la lente et couteuse méthode traditionnelle essai-erreur. L'objectif principal de ce projet consiste à développer des modèles prédictifs permettant d'estimer les attributs géométriques du joint de soudure dans le cas de soudage au laser par recouvrement de tôles en acier galvanisé. L'approche proposée combine expérimentation, modélisation numérique, analyse statistique et modélisation par réseau de neurones pour produire le meilleur modèle prédictif possible. Cette approche est structurée en trois phases.

La première phase a permis de réaliser une investigation expérimentale du procédé dans le but faire une l'évaluation qualitative et quantitative des effets des paramètres et conditions de soudage sur la variation des caractéristiques géométriques de la soudure. Les expériences ont été réalisées à l'aide d'un laser Nd-YAG 3KW à émission continue selon une planification d'expériences basée sur la méthode Taguchi. La seconde phase a permis de développer un modèle de simulation numérique 3D du procédé de soudage au laser basé sur la méthode des éléments finis dans le but de simuler le comportement du procédé dans des

conditions difficiles à réaliser expérimentalement. Le modèle numérique s'appuie sur les équations de transfert thermique en tenant compte des propriétés du matériau dépendant de la température et de l'enthalpie de changement de phase. Le modèle de source de chaleur utilisé a été adapté de manière à modéliser simultanément le soudage en mode conduction et en mode trou de serrure. Les résultats de la première phase ont été utilisés pour la validation du modèle numérique 3D. Dans la troisième phase, on a développé et testé un modèle prédictif en utilisant les réseaux de neurones artificiels. Une large base de données combinant données expérimentales et données de simulation a servi à l'entrainement et à la validation de plusieurs versions de modèles. Plusieurs critères ont été utilisés pour sélectionner le meilleur modèle, pour l'évaluation de la qualité de ses prédictions et sa capacité de généralisation. Les résultats montrent que le modèle obtenu est un modèle de prédiction rapide et robuste présentant des prédictions compatibles avec les mesures expérimentales générant une erreur de prédiction moyenne ne dépassant pas les 7%.

Mots clés : Soudage au laser par recouvrement, laser Nd-YAG, acier galvanisé à faible teneur en carbone, modèles prédictifs, planification d'expériences, méthode des éléments finis, réseau de neurones.

ABSTRACT

Laser welding becomes more and more popular in many industrial fields, including the automotive industry, thanks to its high productivity and flexibility. Due to the focused nature of the laser beam and its high incident power, laser welding is well-known for its high and fast heat input, localized in a very small area, thus promoting the production of deep narrow and aesthetic welds with speeds of up to several cm /s, a very narrow heat affected zone and limited thermal distortions. To deal with the positioning constraints imposed on butt welding and fillet welding, the overlap welding configuration is best suited for large-scale fabrication, but the welding of galvanized steels in this configuration becomes unstable and requires additional precautions, because of the premature vaporization of the zinc coating at the interface of the overlapped parts. An optimal gap between the parts and a better combination of laser parameters can overcome this situation and produce defect free welds.

The mechanical properties of a laser weld seam depend on the shape and dimensions of its cross-section, which themselves depend on the laser parameters and the welding conditions, namely laser power, welding speed, focal diameter and gap. To effectively exploit the benefits of the process, a strategy must be developed to control welding parameters and conditions to achieve welds with desired characteristics, avoiding the slow and expensive traditional test-fail method. The main purpose of this dissertation is to provide a deep understanding of the dependency relationships between welding parameters and weld characteristics. To be able to predict accurately and instantly these characteristics, a three-phase approach is adopted.

The first phase is an experimental investigation of the process, its objective is the qualitative and quantitative evaluation of laser welding parameters effect on the variation of the weld geometry. The experiments are planned according to Taguchi method and conducted using a 3KW continuous Nd-YAG laser on specimens of overlapped galvanized steel sheets. The second phase is the modeling of laser welding process using finite element method, to simulate the process behavior under conditions difficult to perform experimentally. The developed model is based on heat transfer equations and considers temperature-dependent properties of the material and phase change enthalpy. A heat source model is adapted to simulate both laser welding in conduction mode and in keyhole mode. The experimental results are used to validate the 3D finite element model. In the third phase, a large database consisting of experimental results and simulation results is used to train and test a predictive model based on artificial neural networks. Several criteria are used to evaluate the prediction quality of the model and its capacity for future predictions. The obtained results showed a perfect agreement with the experimental measurements, the average prediction error observed is less than 7%.

Keywords: Overlap laser welding, Nd-YAG laser, low carbon galvanized steed, predictive modelling, design of experiments, finite elements method, neural networks.

TABLE DES MATIÈRES

LISTE DES TABLEAUX

LISTE DES FIGURES

INTRODUCTION GÉNÉRALE

Depuis l'invention du premier laser en 1960, plusieurs secteurs industriels se sont penchés sur cette technologie et cherchent à tirer profit de ses avantages. Aujourd'hui, le laser est omniprésent dans notre vie quotidienne, son utilisation s'étend à un nombre infini d'applications et se voit constamment attribuer de nouvelles fonctions. Depuis son avènement dans l'industrie automobile (Fiat 1975), ce secteur a connu une révolution sans précédent, grâce à la multifonctionnalité des robots laser, comprenant le traitement thermique des matériaux, la découpe des métaux et le soudage des pièces de carrosserie. Le soudage laser, qui a fait ses preuves ces dernières années, tend à se substituer au soudage par points par résistance, considéré depuis plusieurs décennies comme le procédé d'assemblage le plus populaire dans l'industrie automobile. Cette transition est due aux nombreux avantages offerts par le soudage laser, tels qu'un faible apport de chaleur, une densité énergétique élevée, une petite zone affectée par la chaleur, une pénétration profonde de la soudure et un aspect très esthétique des cordons de soudure, un rendement très élevé et la possibilité de souder des matériaux peu soudables avec des procédés conventionnels.

0.1 PRINCIPE DE FONCTIONNEMENT DU LASER

Laser est un acronyme anglais qui signifie « Light Amplification by the Stimulated Emission of Radiation » que l'on peut traduire par « amplification de lumière par émission stimulée de la radiation ». Pour comprendre le fonctionnement du laser, il faut plonger dans l'infiniment petit de la matière. Chaque atome est composé d'un noyau entouré d'électrons qui se déplacent autours, répartis sur différentes orbites appelées les niveaux d'énergie. L'apport d'une quantité d'énergie égale à l'écart d'énergie $\Delta \boldsymbol{E}$ entre deux niveaux d'un atome augmente son niveau d'énergie et fait passer un électron d'une orbite à une autre plus élevée;

la molécule est dite alors excitée. Dans le cas du laser, cela est appelé le pompage optique. La molécule ou l'atome va ensuite se désexciter rapidement et l'électron regagne son orbite initiale tout en libérant un photon qui part dans une direction aléatoire c'est ce qu'on appelle l'émission spontanée. Il est possible que le photon libéré rencontre une autre molécule déjà excitée qui va alors l'absorber et se désexciter en émettant deux photons en phase, tous deux de la même longueur d'onde et allant dans la même direction c'est ce qu'on appelle l'émission stimulée. Et comme dans une réaction en chaine, ces photons vont pouvoir exciter d'autres molécules et provoquer d'autres émissions stimulées et ainsi nait un faisceau cohérent monochromatique et unidirectionnel.

La construction des lasers est faite de telle sorte que le faisceau soit canalisé et orienté dans une direction bien déterminée. Pour ce faire, une source laser est constituée d'un milieu actif contenu dans une cavité résonante et d'un système de pompage. Le milieu actif est le milieu dans lequel les rayons lumineux sont produits, qui peut être un cristal (Laser Rubis), un gaz (laser CO2, Laser Argon) ou fibre optique. Le pompage peut aussi se faire de plusieurs façons, soit à l'aide d'un flash lumineux, d'un autre laser ou d'une décharge électrique sur le milieu actif. La cavité résonante est constituée de deux miroirs situés à chacune des deux extrémités du milieu actif. L'un des miroirs réfléchit la totalité de la lumière tandis que l'autre en laisse passer une petite partie, soit 2 à 5%; c'est la sortie lumineuse du faisceau laser. C'est ainsi que les rayons lumineux rebondissent entre les deux miroirs et sont amplifiés à chaque aller-retour. Tout ce processus se déroule très rapidement (à la vitesse de la lumière). Le premier prototype est un laser à rubis développé en mai 1960 par Theodore Maiman [1]. La fibre optique est le moyen utilisé pour le cheminement d'un faisceau laser de la source d'émission jusqu'au lieu de son utilisation.

0.2 TYPES DE LASERS

Selon le type d'émission, on distingue deux types de laser : *laser continu* et *laser à impulsions*. On dit qu'une émission est continue si sa durée dépasse 0.25 seconde, alors que les impulsions durent entre 10^{-15} seconde et quelque dizaine de millisecondes.

Selon le type de milieux actifs, on distingue plusieurs catégories de lasers :

1) Les Lasers à milieu actif solide faits de verre ou du cristal auquel sont incorporés des dopants (ions) qui constituent la partie active du milieu. Le laser Nd-YAG, par exemple, est constitué de grenat d'yttrium et d'aluminium et dopé au néodyme. La longueur d'onde émise par ce laser est de 1064 nm et sa puissance varie de quelques watts à plusieurs Kilowatts.

2) Les Lasers à milieu actif gazeux émettent une longueur d'onde invisible, ils sont souvent utilisés pour la découpe et le soudage des métaux, et ce grâce à leur puissance élevée. Les lasers He-Ne, lasers Kr et les lasers CO2 qui sont les plus courants.

3) Les Lasers à milieu actif semi-conducteur tels que les lasers à diodes sont principalement utilisés dans le secteur de télécommunication.

4) Les Lasers à milieu actif liquide utilisent des liquides actifs (colorants). Leur particularité réside dans la possibilité d'ajustement de la longueur d'onde en modifiant la concentration du milieu actif. Ils ne sont utilisés qu'en mode continu et sont souvent appliqués dans les recherches biomédicales.

0.3 SOUDAGE AU LASER

0.3.1. Avantages et limitations du soudage au laser

Comparé aux procédés de soudage conventionnels, le soudage au laser offre plusieurs avantages :

- Des vitesses de soudage très élevées avec des arrêts et des démarrages rapides.
- La lumière focalisée du laser favorise l'augmentation de la densité d'énergie fournie par la source laser, d'où la possibilité d'obtenir des cordons de soudure fins, profonds et précis et réduire la taille de la zone affectée par la soudure.
- Nul besoin de fixer rigidement les pièces à souder et nul besoin d'un métal d'apport.
- Des matériaux à soudabilité médiocre (titanium, quartz, etc.) peuvent être joints par le procédé de soudage au laser.
- Le procédé de soudage au laser est facile à automatiser et à intégrer à une chaine de production industrielle.

Et comme tout autre procédé, le soudage au laser présente également certains inconvénients :

- En raison du petit diamètre focal qui varie entre 100 et 1000µm, un réglage et un alignement précis des pièces sont beaucoup plus critiques en soudage au laser qu'en soudage à l'arc.
- La qualité de la soudure dépond largement des propriétés de la surface du métal à souder. De plus, les équipements de soudage au laser sont 10 fois plus couteux que les équipements de soudage à arc.
- Et en fin, en termes de la profondeur de pénétration de la soudure, le soudage par faisceau d'électrons prend le dessus [2, 3] .

Les variables indépendantes majeures du processus de soudage au laser incluent la puissance incidente du faisceau laser, le diamètre focal, l'absorptivité et la vitesse d'avance pendant du soudage. Locke et al [4] ont rapporté que la profondeur de pénétration est presque linéairement proportionnelle à la puissance. Le diamètre focal est aussi un paramètre important puisqu'il détermine la densité d'énergie, mais il est difficile à évaluer en raison de la nature gaussienne du faisceau laser. L'efficacité du laser dépend de la capacité du matériau irradié à absorber son énergie, qui à son tour dépend de sa résistivité électrique. Presque tous les métaux ont une faible capacité d'absorption à température ambiante, mais celle-ci augmente considérablement lorsque la température à la surface du métal augmente [5]. La qualité du soudage dépend non seulement de la densité d'énergie du laser, mais aussi du temps d'interaction entre le laser et le métal à souder, c'est-à-dire de la vitesse du faisceau laser (vitesse de soudage). Plusieurs études se sont intéressé à la nature de cette interaction en analysant la corrélation entre la vitesse de soudage et la profondeur de pénétration, mais également le rôle de la vitesse dans la formation et la stabilité du trou de serrure [4, 6].

0.3.2. Modes de soudage au laser

Leong et al. ont développé un modèle mathématique qui permet de prédire le seuil minimal d'irradiance du faisceau laser pour amorcer la fusion sur une surface métallique [6]. Il s'agit d'une simple équation algébrique résultant de la solution de l'équation de flux de chaleur pour une source de chaleur se déplaçant le long d'une plaque. Ce seuil est fonction de la capacité d'absorption de la surface du métal, de sa conductivité thermique, de l'augmentation de la température jusqu'à la fusion, du diamètre du faisceau laser et du rapport de la diffusivité thermique du métal sur le produit du diamètre du faisceau et de la vitesse de soudage [7] .

Il existe une autre valeur seuil, qui est fonction de la densité de puissance (proportionnelle à la puissance du laser et inversement proportionnelle au diamètre du faisceau) et du temps d'interaction du faisceau avec le matériau (fonction de la vitesse de

soudage). Ce seuil représente la limite entre les deux principaux modes de soudage laser, qui sont illustrés par la **figure1**: soudage par conduction et soudage en trou de serrure [8]. D'autres études ont rapporté que ce seuil dépend aussi des propriétés physico-chimiques du matériau et de la longueur d'onde du laser [9, 10] .

Le soudage par conduction est obtenu à une densité inférieure à 10^6 W/cm^2 et à une vitesse supérieure à 8.5 mm/s. À ces niveaux de radiation, le faisceau laser est absorbé par le métal, générant de la chaleur qui est rapidement transférée par conduction et fait fondre les couches surfaciques du métal irradié sans vaporiser le métal fondu. L'observation métallographique des sections transversales de telles soudures révèle un rapport profondeur/largeur inférieur à 4/1. Selon le model développé par Eagar et al., la forme de la section transversale du cordon de soudure obtenu dans le mode conduction est semi-sphérique [11].

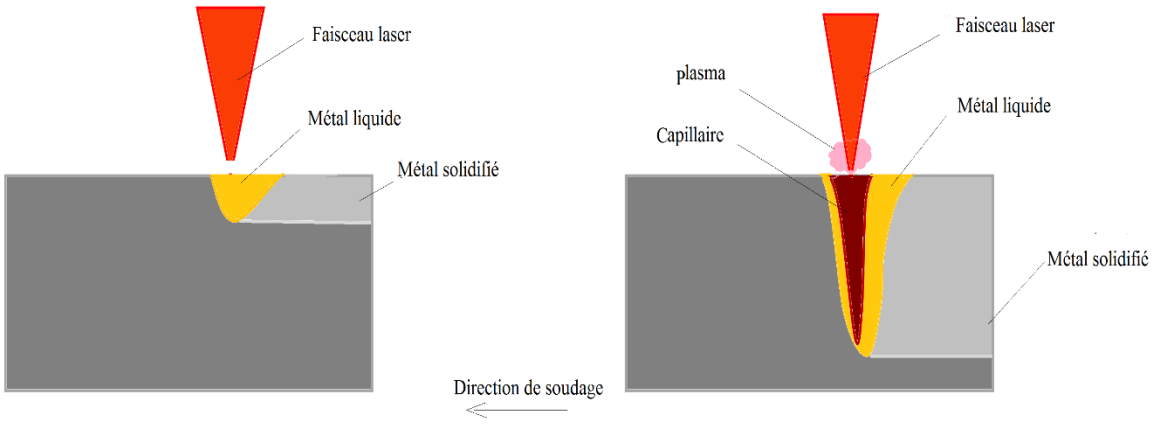

(a) (b)

Figure 1 : Schémas illustratifs du soudage au laser : (a) soudage par conduction (b) soudage en trou de serrure

Les soudures profondes en revanche, nécessitent une radiation supérieure à 10^6 W/cm$^{2.}$ A de tels niveaux de radiation, la vaporisation du métal liquide se produit à travers une épaisseur finie, donnant naissance à une colonne de vapeur métallique entourée de métal liquide, communément appelée cavité de vapeur ou trou de serrure. En raison des gradients de température existant le long des couches liquides de surface et de sous-surface, la tension superficielle varie de façon dramatique pendant que le premier trou de serrure est fondu dans toute son épaisseur. Le métal liquide circule autour de la base du trou de serrure et finit par se solidifier aux bords du capillaire. La stabilité du trou de la serrure est basée sur la densité d'énergie du laser et de la vitesse de soudage. À une densité suffisamment élevée, une vaporisation excessive entraîne la formation de trous de serrure dans toute l'épaisseur du métal, ce qui provoque l'effondrement du métal liquide, comme dans le cas de la découpe au laser. À faible radiation, le métal liquide ne se vaporise pas suffisamment pour pouvoir former un trou de serrure et, par conséquent, la pénétration de la soudure est incomplète. À des vitesses de soudage faibles, la zone de fusion est suffisamment large pour provoquer l'effondrement du métal liquide ; tandis qu'à des vitesses de soudage suffisamment élevées, la pénétration de la soudure est incomplète. L'observation métallographique des sections transversales de telles soudures révèle un rapport profondeur/largeur supérieur à 4/1 [12, 13] .

0.3.3. Configurations de soudage au laser

Les configurations couramment utilisées dans l'industrie automobile lors du soudage laser, comme l'illustre la **figure 2**, comprennent le soudage bout à bout, le soudage par recouvrement et le soudage d'angle [14, 15] .

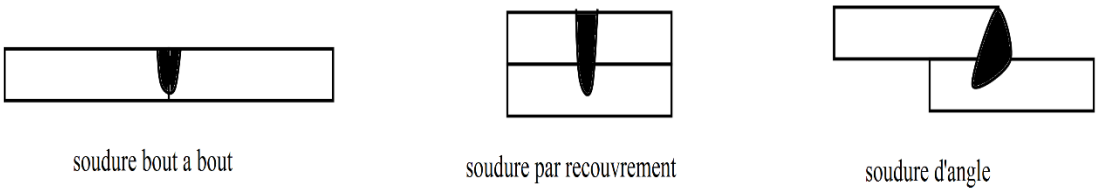

Figure 2 : Configurations de soudage au laser couramment utilisées dans l'industrie automobile

0.4 SOUDAGE PAR RECOUVREMENT DES ACIERS GALVANISÉS

La galvanisation est le procédé de protection abondamment utilisé dans le secteur de l'industrie automobile afin d'améliorer la résistance à la corrosion des composants de la carrosserie automobile. Lors du processus de fabrication et d'assemblage des composants automobile, de nombreux joints de soudure impliquent le soudage par recouvrement des éléments en tôle d'acier galvanisé de diverses épaisseurs et nuances [16] . Le recours à cette configuration de soudage permet de faire face aux contraintes de positionnement précis imposées lors du soudage bout à bout. En effet, le soudage par recouvrement permet d'obtenir des soudures qui ne débordent pas vers l'extérieur et qui sont par conséquent moins sollicitées par la corrosion. De plus, cela donne un aspect externe esthétique à la carrosserie, contrairement au soudage bout à bout qui nécessite des travaux de finition sur les cordons de soudure apparents. Le principal problème du soudage de ces matériaux dans cette configuration, est lié à la basse température de vaporisation du zinc (906 ºC) par rapport à celle de fusion de l'acier (1550 ºC). Pendant le soudage, les revêtements de zinc à l'interface se vaporisent et se dilatent rapidement lorsque le bain de soudure en fusion s'approche de l'interface entre les deux tôles d'acier. Sans jeu entre les tôles, cette vapeur ne peut s'échapper qu'à travers le bain de soudure en projetant du métal fondu à l'extérieur du bain, tandis que

les vapeurs qui n'ont pas réussi à s'échapper, restent piégées à l'intérieur de la soudure après la solidification du métal, sous forme de soufflures, et de contraintes résiduelles [17] .

Certaines approches expérimentales ont été entreprises pour tenter de résoudre ce problème, par exemple en éliminant le zinc à la surface de contact [18], en intercalant des feuilles d'aluminium ou de cuivre le long de la surface de contact des pièces à souder [19, 20], en adoptant un laser à double faisceau [21], en introduisant un arc pour préchauffer le recouvrement en zinc [22], etc. Mais la méthode la plus simple consiste à définir un gap entre les deux tôles superposées pour permettre l'évacuation latérale des vapeurs du zinc. Le gap peut être défini en intercalant des entretoises entre les éléments à souder, ou en réalisant des emboutissages sur l'une des deux tôles [23] . Des travaux récents ont réussi à obtenir des soudures exemptes de défauts, lors du soudage par recouvrement et sans gap seulement par l'optimisation des paramètres de soudage pour permettre l'élongation du trou de serrure [24] ou la pénétration complète de la soudure [25] .

0.5 PROBLÉMATIQUE

Le soudage au laser est de plus en plus employé dans divers secteurs industriels notamment l'industrie automobile et ce grâce à ses innombrables avantages. Aujourd'hui le secteur automobile cherche à réduire la consommation énergétique des véhicules par la réduction de leurs poids, pour se conformer aux normes environnementales qui deviennent de plus en plus restrictives vis-à-vis des émissions en CO_2. Pour une meilleure optimisation du poids d'un véhicule, la nouvelle tendance de conception de la carrosserie automobile consiste à assembler des éléments de tôles de diverses épaisseurs et nuances pour former les composants de la carrosserie, appelés *flancs sur mesure*. Par conséquent, le nombre de soudures dans la carrosserie automobile a plus que doublé lors des deux dernières décennies. Dans ces conditions, l'aptitude des soudures à résister à diverses sollicitations reste la préoccupation principale des ingénieurs.

Le soudage par recouvrement permet d'augmenter le rendement du processus en évitant les contraintes de positionnement qu'imposent le soudage bout à bout et le soudage d'angle. Mais, dans le cas des aciers galvanisés qui sont largement employés dans la construction automobile, le processus devient instable à cause de l'évaporation prématurée du zinc à l'interface des pièces superposées. Plusieurs approches ont été entreprises afin de de remédier à ce problème, et la solution la plus simple et la moins couteuse à intégrer dans le secteur automobile consiste à définir un gap optimal entre les pièces à souder.

Les caractéristiques mécaniques d'une soudure sont directement liées à la géométrie et aux dimensions de sa section transversale, qui est elle-même, fonction des propriétés physico-chimiques du matériau, des paramètres du laser et d'autres conditions de soudage, tel que le gap, qui en plus d'être une alternative pour remédier aux problèmes liés aux vapeurs de zinc, peut être une source de variation des caractéristiques de la soudure. L'industrie automobile a donc besoin d'exploiter efficacement les avantages du soudage au laser par recouvrement des aciers galvanisés et mettre en place des stratégies qui permettent de contrôler les paramètres et les conditions de soudage de sorte à obtenir les recettes les plus fiables et les plus rentables. L'optimisation du processus basée sur la méthode traditionnelle essai-erreur est non seulement lente et couteuse, mais elle ne fournit pas non plus une compréhension du comportement du procédé, étant données sa complexité et la multitude des phénomènes physiques qui le constituent. Dans ce sens, le recours à la modélisation est nécessaire pour être en mesure non pas seulement d'analyser le procédé et comprendre ses particularités et ses limites mais également de prédire son comportements et les caractéristiques des soudures qu'il est capable de produire en fonction de l'ensemble de ses paramètres.

Plusieurs types de modélisation peuvent être considérés dans le cadre de ce projet, Cependant, lorsqu'on cherche à prédire plusieurs caractéristiques dépendant de plusieurs variables, les modèles à base de réseaux de neurones artificiels offrent de avantages par rapport à d'autres types de modèles empiriques notamment les différents types de régressions. Dans le cas de modélisation prédictives, les modèles numériques sont très lents

et inappropriés [26]. De plus, les modèles par réseaux de neurones ont déjà été utilisés avec succès pour modéliser de nombreux procédés de soudage [26]. Toutefois, le développement de tels modèles nécessite des données riches et abondantes pour garantir l'efficacité et la crédibilité des processus d'apprentissage et de validation [26-29]. Les données expérimentales étant relativement couteuses à produire, un modèle de simulation 3D basés sur la méthode des éléments finis peut être utilisé pour générer une partie des données pour la modélisation prédictive. Evidemment, les différents modèles numériques ou neuroniques doivent être validés par des données qui proviennent de l'expérience.

0.6 OBJECTIFS ET MÉTHODOLOGIE

Le présent projet constitue une étude du soudage au laser par recouvrement d'un acier galvanisé faiblement allié au carbone, largement employé dans la construction automobile. L'objectif principal de ce projet consiste à développer un modèle simple, précis et efficace capable de prédire les attributs géométriques du joint de soudure dans le cas de soudage au laser par recouvrement de tôle en acier galvanisé faiblement allié. Ce type de modèle est susceptible de fournir à l'industrie automobile un outil de prédiction permettant de réduire substantiellement les temps et les coûts de réglage durant la production des assemblages soudés. Pour atteindre cet objectif, une approche en trois étapes est adoptée :

La première phase consiste à réaliser une investigation expérimentale du soudage au laser par recouvrement d'un acier faiblement allié au carbone (ASTM A635 CS) avec un revêtement galvanisé A40, en utilisant une source laser Nd-YAG 3 KW, sur la base d'un plan expérimental structuré selon la méthode Taguchi. Cette investigation porte essentiellement sur l'identification, l'évaluation et l'analyse des effets de divers paramètres et conditions de soudage sur la variation des caractéristiques géométriques et mécaniques de la soudure. Des outils statistiques éprouvés tel que l'analyse de la variance constituent l'un des ingrédients de base de cette analyse. La variation des caractéristiques géométriques du joint de soudure telles que la profondeur de pénétration de la soudure (DOP), la largeur du cordon de soudure

à la surface de la plaque supérieure (WS) et la largeur du cordon à l'interface (WI) est évaluée en fonction de la variation des paramètres tels que la puissance du laser, la vitesse d'avance du faisceau laser, le diamètre focal ou encore l'écart entre les tôles.

La deuxième étape consiste à développer et à valider expérimentalement un modèle numérique 3D capable de simuler le comportement du procédé sous des conditions difficiles à réaliser expérimentalement. Le modèle 3D est développé sur un logiciel commercial de simulation (COMSOL) utilisant la méthode des éléments finis. Le modèle en question est basé sur les équations de transfert de chaleur et tient compte des propriétés thermo-physiques du matériau et de son enthalpie de fusion. Une source de chaleur gaussienne adaptative est utilisée pour simuler à la fois le comportement du faisceau laser dans les modes de soudage conduction et trou de serrure. L'utilité d'un tel modèle réside dans la production de données à bas coût permettant à la fois de raffiner l'analyse des effets de divers paramètres et conditions de soudage sur la variation des caractéristiques géométriques et mécaniques de la soudure et de générer une base de données suffisamment riche, diversifiée et robuste pour constituer un des fondements de la modélisation prédictive par réseaux de neurones artificiels.

Finalement, la troisième phase consiste à développer un modèle de prédiction rapide, précis et robuste capable de prédire les attributs géométriques du joint de soudure peu importe les paramètres et les conditions de soudage. Le choix du type de modèle et la sélection des variables à y inclure sont deux éléments clés à considérer. Grâce à leur forte capacité d'apprentissage et de généralisation, les modèles à base de réseaux de neurones sont capables de prendre en charge les relations complexes et hautement non linéaires entre les variables du procédé de soudage au laser. Le perceptron multicouche avec propagation en arrière s'avère le type de réseau neuronique le mieux adapté pour la prédiction dans la présente application. Le choix des variables à inclure dans le modèle est basé sur l'analyse de leurs contributions dans la précision et dans la robustesse des modèles qu'elles supportent. Plusieurs modèles représentant de nombreuses combinaisons de variable sont développés et testés. La contribution des différentes variables à l'amélioration de la qualité de prédiction

est évaluée en utilisant ANOVA. Les données nécessaires pour l'entrainement et la validation des modèles développés, sont extraites d'une part des mesures expérimentales et d'autre part des prédictions faites par le modèle 3D. Deux différentes méthodes de validation sont utilisées pour évaluer la capacité de chaque modèle à faire des prédictions futures, et finalement définir lequel des modèles est le meilleur.

0.7 ORGANISATION DU MÉMOIRE

Le présent mémoire se compose de trois chapitres, rédigés sous formes d'articles. Le premier article présente une investigation expérimentale du soudage au laser par recouvrement d'un acier galvanisé à faible teneur en carbone, communément utilise lors de la fabrication de la carrosserie automobile. Les expériences sont réalisées à l'aide d'un laser à émission continue de type Nd-YAG 3 KW en suivant un plan d'expérience structurée selon la méthode Taguchi. Une série de tests préliminaires est conduite pour définir les limites inférieures et supérieures des paramètres du laser, soient la puissance du laser, la vitesse de soudage, le diamètre et du faisceau et le gap, de telle manière à obtenir des soudures sans défauts et une fusion qui dépasse l'interface mais sans déborder par la surface inférieure. Ainsi, les effets des différents facteurs sur la variation des attributs géométriques de la soudure sont évalués à l'aide d'outils statistiques pertinents.

Le deuxième article présente une approche de modélisation du processus de soudage au laser, par la méthode des éléments finis, en se basant sur les équations de transfert de chaleurs, les propriétés thermo physiques du matériau et l'enthalpie de changement de phase. Les profils thermiques obtenus lors des simulations numériques permettent de déduire les dimensions et les formes de la soudure pour plusieurs combinaisons de paramètres de soudage. Le troisième article, présente un modèle de prédiction par réseaux de neurones artificiels, un modèle rapide et hautement précis, développé et entrainé à l'aide d'une base de données robuste générée par le modèle 3D.

CHAPITRE 1
INVESTIGATION EXPERIMENTALE DU SOUDAGE AU LASER PAR RECOUVREMENT

1.1 RÉSUMÉ EN FRANÇAIS DU PREMIER ARTICLE

L’article présente une investigation expérimentale du soudage au laser par recouvrement de l’acier galvanisé à faible teneur en carbone. Basée sur un plan expérimental structuré suivant la méthode Taguchi, l’investigation est axée sur l’évaluation de des effets des paramètres de soudage au laser sur la qualité des soudures. Les expériences de soudage sont réalisées à l'aide d'une source laser Nd-YAG de 3 kW. Les paramètres de soudage au laser considérés (puissance laser, vitesse de soudage, diamètre de la fibre laser, gap entre les feuilles et leurs épaisseurs) sont utilisés pour évaluer la variation de trois caractéristiques géométriques de la soudure (profondeur de pénétration, largeur du cordon à la surface et largeur du cordon à l'interface). Des outils statistiques améliorés sont utilisés pour analyser les effets des paramètres de soudage sur la variation de la qualité de la soudure et pour identifier les relations possibles entre ces paramètres et les caractéristiques géométriques de la soudure. Les résultats montrent que les valeurs de dureté atteintes sont similaires pour tous les tests expérimentaux et que tous les paramètres de soudage contribuent pertinemment à la variation de la qualité de la soudure avec une prédominance relative de la puissance laser et de la vitesse de soudage. L'effet du gap est relativement limité. Les résultats de l'étude révèlent également qu'il existe de nombreuses options à prendre en compte pour créer un modèle efficace de prédiction de la qualité des soudures. Les résultats obtenus à l'aide d'un modèle simplifié basé sur les réseaux de neurones artificiels fournissent une indication sur les performances du modèle de prédiction.

Ce premier article, intitulé « *Exeprimental investigation of laser welding in the overlap configuration* », fut rédigé par moi-même ainsi que par le professeur Abderrazak El Ouafi et le professeur Ahmed Chebak. Il a été publié en 2019 dans la revue *Journal of Materials Science and Chemical Engineering*. En tant que premier auteur, ma contribution à ce travail fut l'essentiel de la recherche sur l'état de l'art, le développement de la méthode, l'exécution des tests de performance et la rédaction de l'article. Le professeur Abderrazak El Ouafi, second auteur, a fourni l'idée originale. Il a aidé à la recherche sur l'état de l'art, au développement de la méthode ainsi qu'à la révision de l'article. Ahmed Chebak, troisième auteure, a contribué au niveau de la méthode et à la révision de l'article.

1.2 ABSTRACT

This paper presents an experimental investigation of laser overlap welding of low carbon galvanized steel. Based on a structured experimental design using the Taguchi method, the investigation is focused on the evaluation of various laser welding parameters effects on the weld's quality. Welding experiments are conducted using a 3 kW Nd-YAG laser source. The selected laser welding parameters (laser power, welding speed, laser fiber diameter, gap between sheets and sheets thickness) are combined and used to evaluate the variation of three geometrical characteristics of the weld (penetration depth, bead width at the surface and bead width at the interface). Various improved statistical tools are used to analyze the effects of welding parameters on the variation of the weld quality and to identify the possible relationship between these parameters and the geometrical characteristics of the weld. The results reveal that the reached hardness values are similar for all the experimental tests and all welding parameters are relevant to the weld quality with a relative predominance of laser power and welding speed. The effect of the gap is relatively limited. The investigation results reveal also that there are many options to consider for building an efficient welds quality prediction model. Results achieved using an artificial neural network based simplified model provide an indication of the prediction model performances.

1.3 INTRODUCTION

Laser welding is more and more gaining place against resistance spot welding, which is considered as the most popular joining process in the automotive industry for several decades. This transition is due to many advantages of laser welding such as low heat input high energy density, small heat affected zone, fast welding and deep penetration as well as esthetic weld seams. Sheets with different alloys, shapes, thicknesses or material properties can be welded using laser. However, to improve the corrosion resistance of the vehicle parts

in automotive industry, various coatings alternative can be considered. Among these techniques, zinc surface coating is the most popular [30] . Due to the low boiling temperature of the zinc (1180 K) compared to the fusion temperature of steel (1808 K), the laser welding process of galvanized steel in the overlap configuration exhibits instabilities. This is caused by the premature vaporization of the zinc coating at the sheets interface generating a high pressures ranging from 50 to 100 bars at temperatures varying from 1800 to 2000 K [24]. The pressurized vapors disturb the welding process by ejecting the molten metal outside the melt pool, and zinc vapors can be trapped in the weld after solidification, as blowers and spatters [31]. Various studies are conducted for understanding the chaotic behavior of the zinc during laser welding process. Fabro et al. [24] reported that zinc vapors flow first into the keyhole and then expand rapidly in the volume of the molten metal, creating a jet of gas that disrupts the molten flow. A study of the dynamics of the liquid zinc flow between the overlapped sheets during laser welding process, suggests that the zinc moves away from the fusion zone when metal is liquid and moves back to the weld pool after solidification [32] . Norman et al. described three modes of defects evolution during welding and presented the main causes of various defects types [33, 34]. Many approaches are proposed to overcome the zinc related problems and improve the weld joint quality. Providing a gap between the sheets allows a lateral escape of zinc vapors without affecting the weld pool. Therefore, the selection of optimal gap can lead to defect free welds [23] . In contrast, an inappropriate gap reduces the weld quality. In fact, a very small gap is not sufficient to release the vapor, while a large one does not allow the fusion of the two parts to be welded together [35]. A study of the laser overlap welding process behavior of galvanized steels reported that a gap ranging from 0.04 to 0.15 produces high strength and homogenous welds [36] . To produce acceptable welds, Akhter et al. [18] proposed a simplified model illustrated by equation below to estimate the size of the required gap from the volume of the zinc vapor to be exhausted. However, the difficulty to maintain a constant gap along the weld line remains unresolved.

$$g = kvt_{zn}t_p^{1/2}$$

Where, g is the gap, k is material constant, $t_{zn}$is the zinc coating thickness and t_p is sheet thickness and v is the welding speed.

Several other methods, using additional elements that can interact with zinc before its evaporation, such as copper or aluminum have been tested [37]. Although these elements contributed to the stability of the laser welding process, some of the added elements affected negatively the mechanical properties of the weld. Mechanical removal of the zinc coating layer before welding leads to a good weld quality while losing the resistance to corrosion [37]. Furthermore, those methods require additional production costs or added manufacturing steps for an industrial scale generalization. Several experimental studies are conducted to evaluate the weld quality in a non-destructive manner [25] [38-41]. Sinha et al. investigated the relationship between the variation in weld bead width, measured at the top surface of the lap welded joint, and the mechanical properties of the weld bead, as well as the effects of the gap and other welding parameters on this variation [38]. This study reported that a wide width variation reflects a poor quality of the weld. Zhao et al. conducted an experimental study in order to evaluate the effects of laser welding parameters on the weld bead geometry in the overlap configuration of thin-gauge galvanized steels by using response surface methodology [39]. It was demonstrated that an optimal combination of these parameters increases the aspect ratio of the weld joint by 30%. Wei et al. reported that the increase in laser power makes it possible to switch from the conduction welding mode to the keyhole mode [40]. Consequently, the keyhole mode can be considered as a degassing channel, but the deals lies in the stability of the keyhole during the welding process. Elongating the keyhole in order to facilitate the zinc vapor escape can be achieved by defocusing the laser beam, by tilting it, or by using multiple laser spots [41]. Fabro reported that an elongated keyhole improves weld quality with CO2 laser beam but not with Nd-YAG laser source [24]. A fast frequency modulation of laser power allows partial reduction of zinc-related defects during lap welding of galvanized steels [41]. Using an optimum speed-power combination, Pieters and Richardson reveal that defect free welds can be achieved in overlap configuration without gap or special manipulation technique. This is possible only with full penetration mode [25]. Based on these remarks, it is obvious that a good quality welds during overlap laser welding

of galvanized steels depends on the adjustment of the laser parameters and the size of the gap between the sheets. A structured experimental design combined to improved statistical analysis tools can provide a deep understanding of the effects of laser parameters, welding conditions and their interactions on the variation of the geometrical and mechanical characteristics of the welded joints and can conduct to efficient and robust model for predicting the welds quality. This paper presents an experimental investigation of overlap laser welding of zinc coated low carbon steel. Based on a structured experimental design, the investigation is focused on the evaluation of the effects of various laser welding parameters and conditions on the variation of the geometrical and mechanical characteristics of the weld quality.

1.4 EXPERIMENTATION

1.4.1 Parameter identification

The experimental investigations are conducted using ASTM A635CS galvanized steel with A40 coating type. Three sheet thicknesses varying from 0.8 to 3.6 mm are selected for the experimentations to conform to the thickness range commonly used in the automotive industry. The sheet specimens having 1, 2 and 3 mm thickness are cut using hydraulic shear at the size of 30 × 50 mm. The sheets are then superimposed two by two to perform the laser overlap welding. **Table 1** illustrates the chemical compositions of the used sheets provided by the steel manufacturer. Note that the very small variations in chemical composition are neglected. Laser power (P), welding speed (S), laser spot diameter (D) and Gap (G) are the considered parameters in this experimental investigation. The upper and lower limits of these parameters are set using some results from the conducted preliminary tests and others relevant information extracted from the related literature.

Table 1 : Chemical composition of the used material

Sheet thicknesses	C	Mn	P	S	Si	Cu	Ni	Cr	Al	N
3 mm sheet	0.04	0.19	0.005	0.002	0.01	0.01	0.02	0.009	0.038	0.0039
2 mm sheet	0.09	0.35	0.005	0.01	0.02	0.05	0.04	0.06	0.03	0.0029
1mm sheet	0.05	0.24	0.009	0.013	0.007	0.029	0.012	0.037	0.04	0.0024

1.4.2 Experimental Setup

The experimental investigation is carried out using a welding laser cell composed of a FANUC M-710iC six-axis robot, directing a laser beam coming from a HIGHYAG BIMO laser head powered by an IPG YLS-3000-ST2 fiber laser source. The laser power is transferred through an optical fiber with a diameter of 200 µm. The maximum power that can be emitted by the Nd-YAG laser source is 3 KW with a wavelength of 1070 nm. The laser head is equipped with a variable-zoom collimator and a fixed focusing lens. The collimator adjustment provides circular focal spots with a diameter ranging from 340 to 520 µm, for a focal length of 300 mm. **Figure 3** shows the used laser welding setup for the experimentations.

Figure 3 : Laser overlap welding setup

After welding, the samples are processed following a standard metallography procedure: 1) cutting assemblies perpendicular to the weld to obtain the desired cross section, 2) specimens' preparation for microscopic observation including grinding polishing, etching and finally 3) microscopic observation using a CLEMEX MMT Type A microscope. The microscope is equipped with contour identification programme permitting the evaluation of the weld geometrical attribute in the cross section.

As defined in **Figure 4**, the measured weld dimensions are the depth of penetration (DOP), bead width at the surface (WS) and bead width at the interface (WI). Each measurement was taken three times and then averaged to constitute the database used for the statistical analysis. Vickers micro-hardness testing is also conducted using a load of 500 g and a dwell time of 15 s. The base material measurements are taken far from the fusion zone.

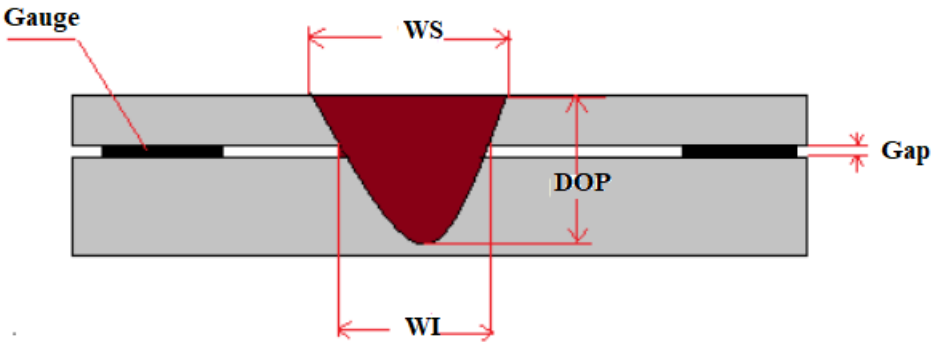

Figure 4 : Geometric characteristics of weld cross section in overlap configuration

1.4.3 Preliminary Tests

Due to the anticipated difficulties related to the zinc vapors present at the interface of the parts during overlap welding of galvanized steels, preliminary tests are carried out in order to define the range of variation of the gap to achieve welds with a good visual appearance and to set the upper and lower limits of laser welding parameters to reach depths exceeding the interface without breaking down the bottom sheet. By varying one parameter at a time the combination of maximum power-minimum speed-minimum diameter produces the maximum deep-seam weld (3 mm), while the reverse combination produces a weld at the minimum depth (1 mm), so the min/max limits for each of the settings are obtained; i.e. 2000/3000 W for the power, 40/70 mm/s for the speed and 300/490 µm for the diameter. It is also found that welds with acceptable visual aspect are obtained with gap ranging from 0.05 mm to 0.15 mm.

1.4.4 Design of Experiments

Factorial designs are the simplest experimental designs to use. They provide the maximum data on the process to be studied. However, the number of necessary tests grows exponentially as soon as an additional factor or level are introduced to the design, making the experience more expensive and more time consuming. However, fractional plans achieve fewer tests and allow a very good ratio between experimental cost and generated data. For this reason, an experimental design is established according to the Taguchi method. An L9 matrix consisting of three factors at three levels aims to examine the impact of the selected laser welding parameters on the geometrical characteristics of the weld cross section. The choice of three levels for each factor is proposed in order to study the linearity of factors effects on the weld geometry characteristics. Laser parameter levels are identified in **Table 2** and the experimental design is presented in **Table 3**.

To understand the effect of the interface and that of the gap size on the variation of the shape and the dimensions of the weld, two experimental variants are suggested to conduct the proposed designs. The first variant consists to use the 3 mm thickness sheet alone by passing the laser beam along the sheet surface in order to evaluate the size of the melted zone without any joining. This variant constitutes the first L9 design. The second variant consists to replace the 3 mm thick sheet by two superimposed sheets of 1 mm and 2 mm thicknesses respectively and reproduce the same experimental design, but this time for performing overlapping welds. This experimental variant is reproduced three times using three gap values (0.05 mm, 0.1 mm and 0.15 mm). For that, gauges of different thicknesses are interposed between the sheets to form a gap allowing lateral evacuation of the zinc vapors present at the interface. The zinc vapors are known to have disruptive effects on the overlap welding process of galvanized steels. Therefore, three based gap L9 matrices are used.

Table 2 : Factors and levels for the experiments

Factor	**Level 1**	**Level 2**	**Level 3**
Power (W)	2000	2500	3000
Welding speed (mm/s)	40	55	70
Focal diameter (µm)	300	395	490

table 3: L9 design of experiments

Tests	**Power (W)**	**Speed (mm/s)**	**Spot diameter (µm)**
1	2000	40	300
2	2000	55	395
3	2000	70	490
4	2500	40	395
5	2500	55	490
6	2500	70	300
7	3000	40	490
8	3000	55	300
9	3000	70	395

1.4.5 Repeatability Tests

In order to establish a measurement quality reference, 8 repeatability tests are done using the median values used in the experimental design (2500 W for power, 55 mm/s for speed, 395 µm diameter and 0.1 mm for gap). To estimate the total measurement error due to the uncontrolled factors, such as maintaining a constant gap along the welding line applying the same conditions during welding, an average of the quality attributes, standard deviations and relative errors are estimated. The results summarized in **Table 4** present a very good repeatability. The variations are less than 10%. These results ensure the measurement method validity and prepare for the experimentation phase with confidence.

Table 4: Repetability test results

Quality attributes	**DOP (µm)**	**WS (µm)**	**WI (µm)**
Max	1341	1336	1288
Min	1317	1209	1254
Mean	1329	1248	1269,5
Std-deviation	7.76	43.74	11.94
Relative error	1.8%	10%	2.7%

1.5 RESULTS AND DISCUSSION

1.5.1 Evaluation of the Laser Parameter Effects

Globally, the produced welds present acceptable visual characteristics, nevertheless some discontinuities of the welds and some projections of the metal observed in the case of certain samples representing experiments with 0.05 mm gap. **Figure 5** presents typical welds achieved using P = 3000 W, S = 70 mm/s, D = 395 mm and G = 0.05 mm. The experimental data are analyzed using three statistical tools: the graph of the average effect for each factor, the percent contribution of factors extracted from the analysis of variance (ANOVA) and the correlation between various weld characteristics and laser parameters. The percent contribution of a factor reflects the portion of the total variation observed in the experiment that is attributed to that factor. Ideally, the total percent contribution of all considered factors must add up to 100. Any difference from 100 represents the contribution of other uncontrolled factors and experimental errors. As the experiments are designed using an OA, the estimates of the average effect of a given factor on various responses will not be biased.

The experimental results extracted from the 3 designs related to the overlap laser welding with a gap, respectively of 0.05, 0.1 and 0.15 mm are averaged in an L9 Taguchi design, and then analyzed using the three statistical tools: graph of effects percent contribution and correlation between geometric characteristics of the welds and laser welding parameters.

ANOVA results in **Table 5** and graphs of average effects in **Figure 6** show that the laser power has positive effect on the variation of the weld characteristics. This effect is almost linear on DOP and WS and non-linear on WI. The contribution of the power in WS variation is 50% against 40% in WI variation and 14% for DOP. A nonlinear and significant negative effect of the welding speed on the variation of the three studied weld properties is observed.

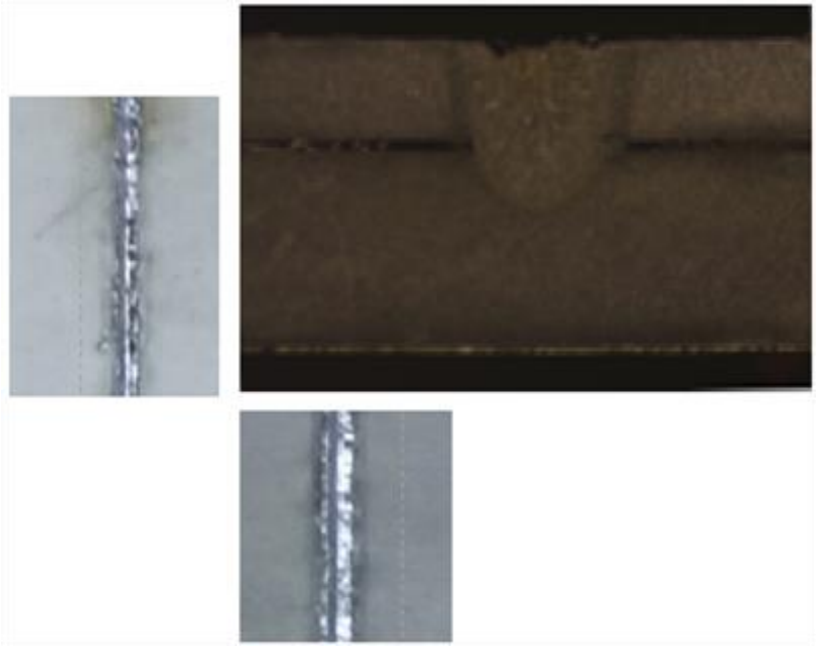

Figure 5 : Typical cross section shape of overlap laser welded galvanized sheets

The speed contribution in DOP variation is 71%, against 37% for WS and 40% for WI. The effect of the laser spot diameter is not very important with negative effect on DOP variation and a contribution of 13%. The laser spot diameter contribution in WS variation is 12%. Its effect on WI variation is positive for small diameters and negative for large diameters with 13% of contribution.

The previous observations are confirmed by the correlation's analysis between geometrical attributes of the weld and laser welding parameters presented in **Table 6**. A very significant correlation between the welding speed and the different characteristics of the weld is observed. The focal diameter presents a weak correlation with weld dimensions with correlation coefficients less than 30%. Laser power is strongly correlated with the WS. As expected, strong correlations are observed between different weld characteristics.

Table 5: ANOVA of averaged weld dimensions results

Source	DOP		WS		WI	
	F-value	**C %**	**F-value**	**C %**	**F-value**	**C %**
Power	5.76	13.88	131.01	50.23	7.25	39.34
Speed	29.80	71.72	97.2	37.26	7.45	40.45
Diameter	4.98	12	31.63	12.12	2.73	14.79
Error		2.41		0.38		5.43

Table 6: Correlation between laser parameters and weld dimensions

Correlation (%)	Power	Speed	Diameter	DOP	WS	WI
DOP	37	82	20	100	-	-
WS	70	60	26	65	100	-
WI	57	62	29	78	72	100

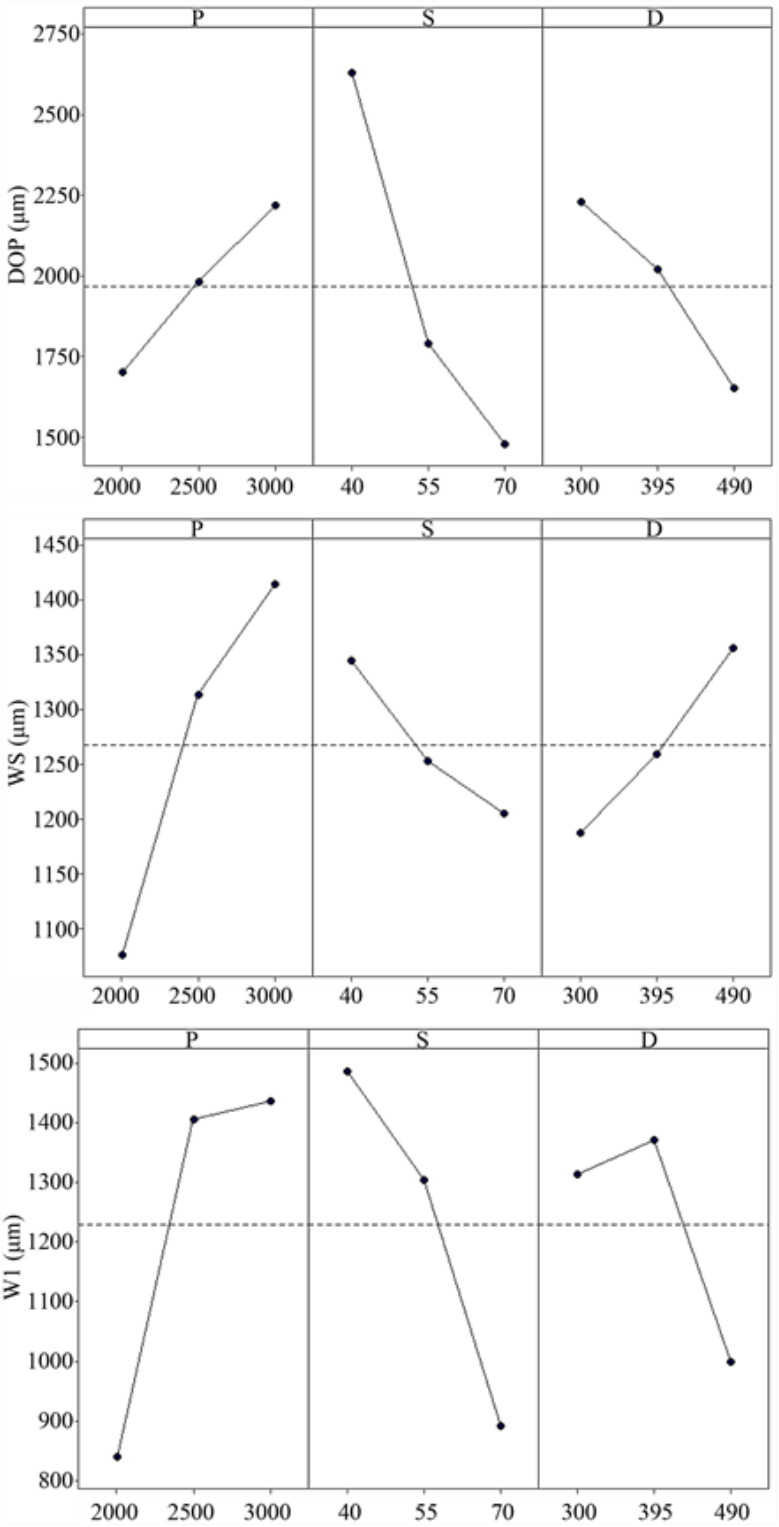

Figure 6 : Graphs of average effects of laser welding parameters on weld dimensions

1.5.2 Evaluation of the Gap Effects

An L27 orthogonal array using four three-level factors is formed from three L9 blocks to allow the integration of the gap factor into an extended design. ANOVA results in **Table 7** and graphs of average effects in **Figure 7** show a relatively limited effect of the gap on the variation of different weld geometrical characteristics. The maximum contribution of the gap is observed on DOP variation by 7.3%.

Figures 8-10 present the effects of the interface and the gap size on the contributions of the laser welding parameters (power, speed and diameter) in the variation of the weld geometrical characteristics.

Table 7 : ANOVA results performed on the L27 blocked design

Source	**DOP**		**WS**		**WI**	
	F-value	**C %**	**F-value**	**C %**	**F-value**	**C %**
Power	5.76	13.02	226.70	46.98	40.43	37.35
Speed	29.80	67.28	168.18	34.85	41.47	38.40
Diameter	4.98	11.25	31.63	11.34	15.17	14..04
Gap	7.38	3.81	23.54	4.96	2.02	1.87
Error		4.64		1.87		8.33

These values are extracted by comparing the results obtained from the four designs for understanding the effects of the interface and the gap size on the weld quality. In these figures, it can be observed that the presence of the interface does not affect the percentage of contribution of laser power in the variation of weld dimensions, but a small gap considerably

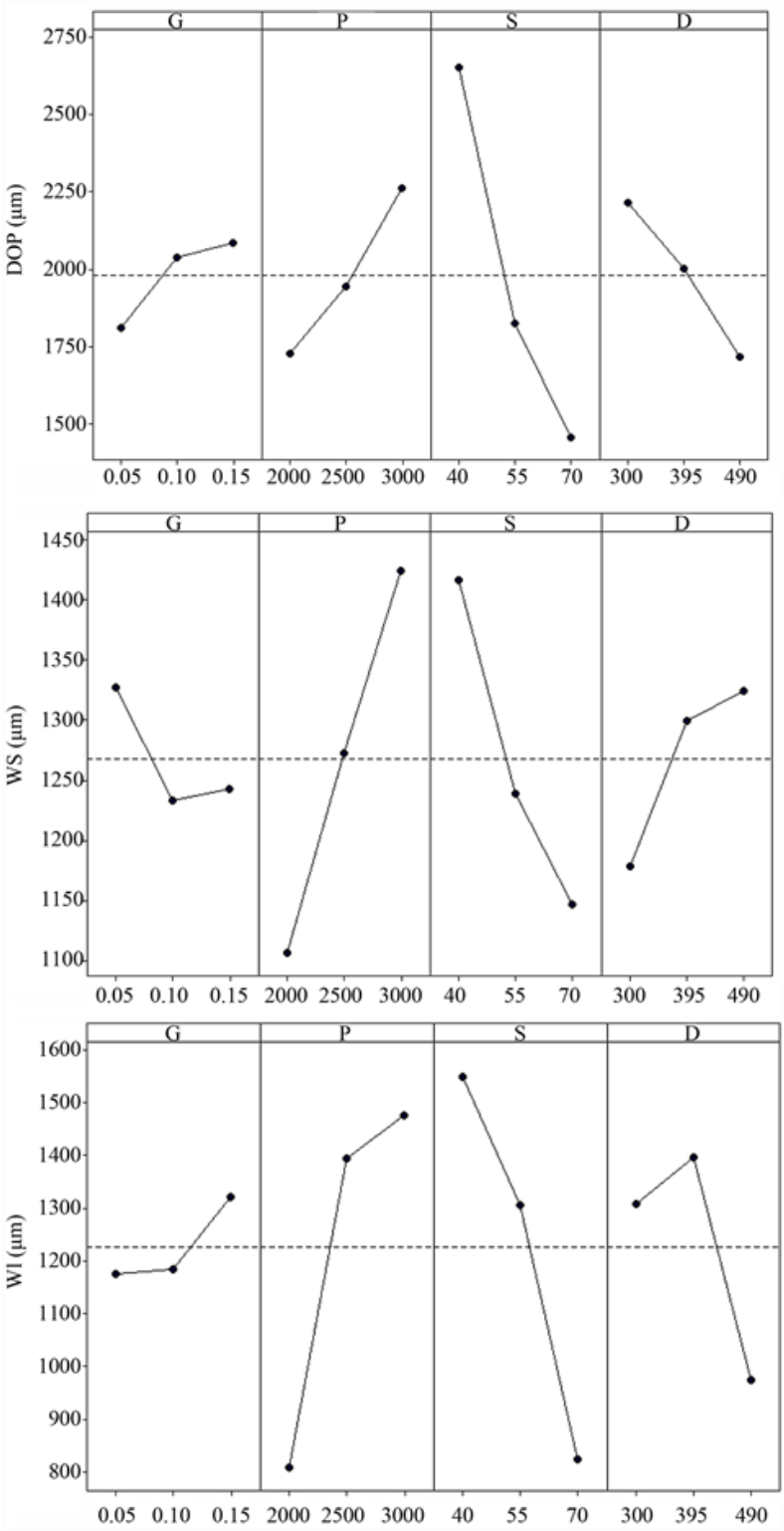

Figure 7 : Graph of effects of laser welding parameters including Gap.

reduces the contribution of laser power in WI variation, and a wide gap decreases the contribution of laser power in DOP variation. The presence of the interface increases drastically the contribution of the welding speed on WS and WI variations, whereas the contribution in DOP variation is slightly affected.

The contribution of speed in the variation of the weld dimensions is almost insensitive to the size of the gap. The contribution of the focal diameter in DOP variation is also insensitive to the interface and the gap size, while its contribution in WS variation is negatively affected by the presence of the interface and by the gap size. The percentage of contribution of laser spot diameter in WI variation increases considerably in the presence of the interface and decreases by increasing the gap size.

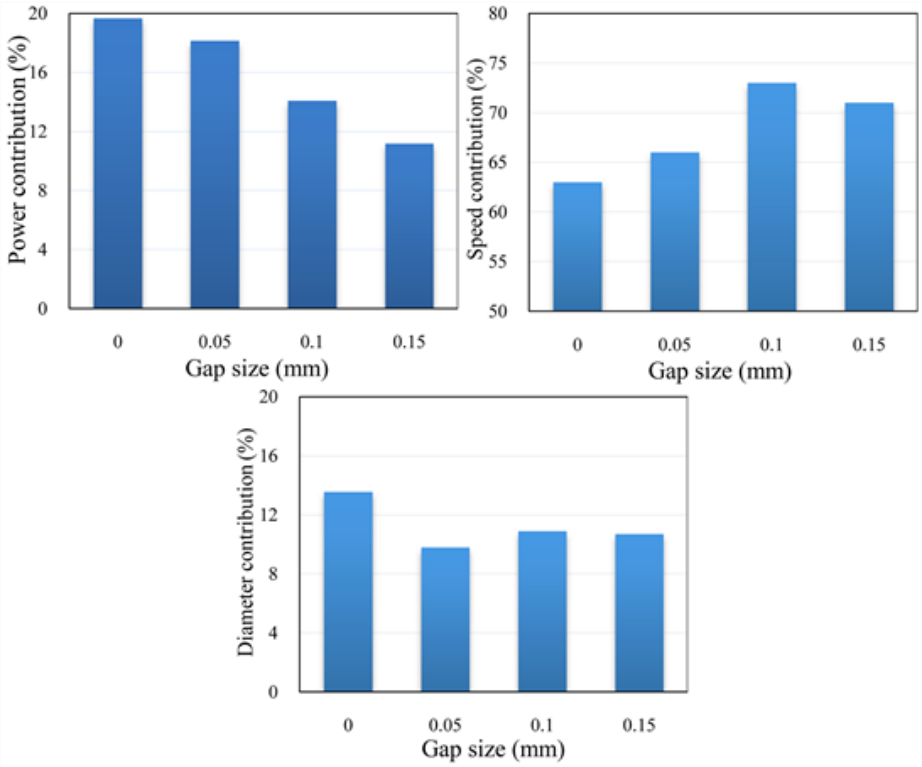

Figure 8 : Percentage contribution of laser welding parameters in DOP variation

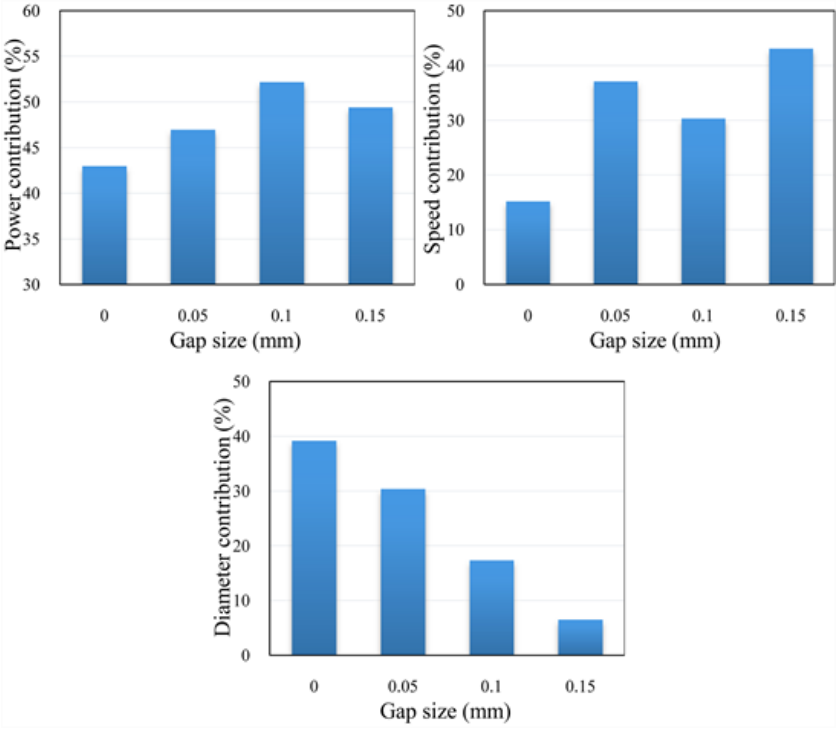

Figure 9 : Percentage contribution of laser welding parameters in WS variation

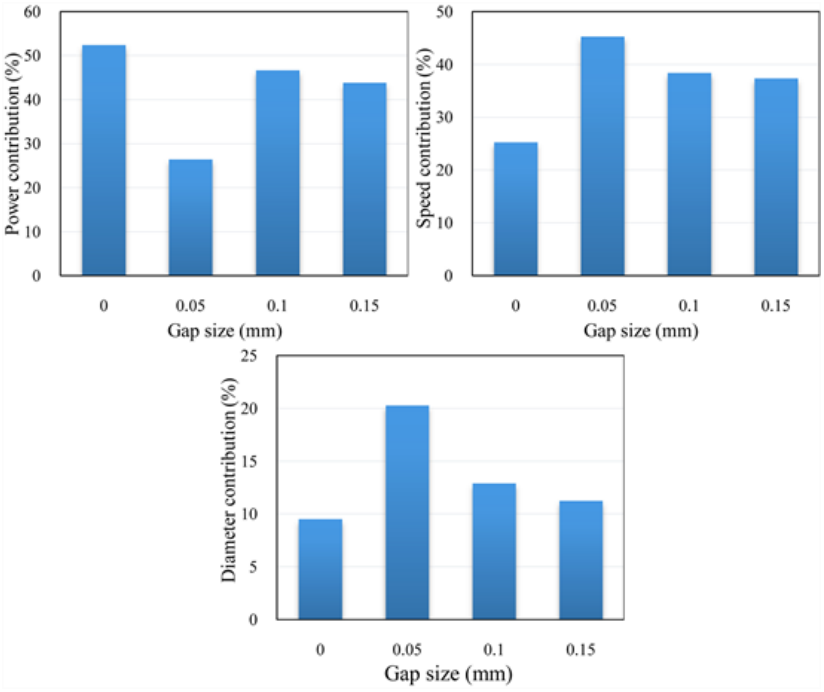

Figure 10 : Percentage contribution of laser welding parameters in WI variation

1.5.3 Micro Hardness

Figure 11 shows the hardness profile in the penetration direction of the weld. The hardness test shows coherent results with an increase in the weld hardness from 150 Hv (hardness of base metal) to 250 Hv (hardness recorded on the cross section of the weld bead).

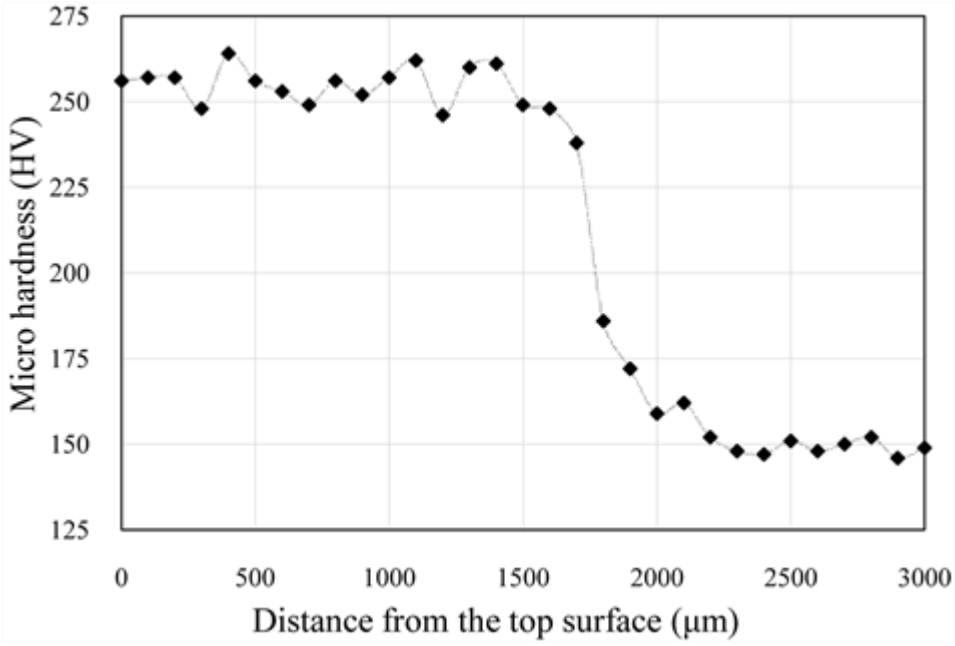

Figure 11: Hardness profile of welded sheets

1.5.4 Simplified ANN Prediction Model for Weld Dimensions

The laser welding parameters that have important effects on weld quality variation are identified. Weld characteristics exhibit a complex and nonlinear relationship with specific parameters. To be able to implement an effective prediction approach, it is necessary to develop an efficient and robust model. Although several techniques can be used to produce such a model, artificial neural networks (ANN) have been proven to be an effective tool for this type of applications [28, 42]. Thus, ANN is chosen in this study for an illustrative example of weld dimensions prediction model. The experimental data from the three L9 design is used to train the ANN based prediction model. The experimentation results suggest

that power, speed, fiber diameter and gap are the largest contributors to the geometrical weld characteristics variation (DOP, WS and WI). Consequently, P, S, D and G are used as input to the predictive model. The modelling results demonstrate that the models can accurately predict the weld characteristics with an error less than 12%. The measured and predicted DOP, WS and WI are shown in **Figure 12**. These results suggest that the modeling approach can be effective for weld quality prediction. A more accurate definition of the weld quality attributes, an experiment covering more laser welding parameters and more factor levels for more training and validation data as well as an improvement of the modeling procedure can lead to more accurate and efficient models. This may probably lead to model improvement decreasing the modelling error to less than 5%.

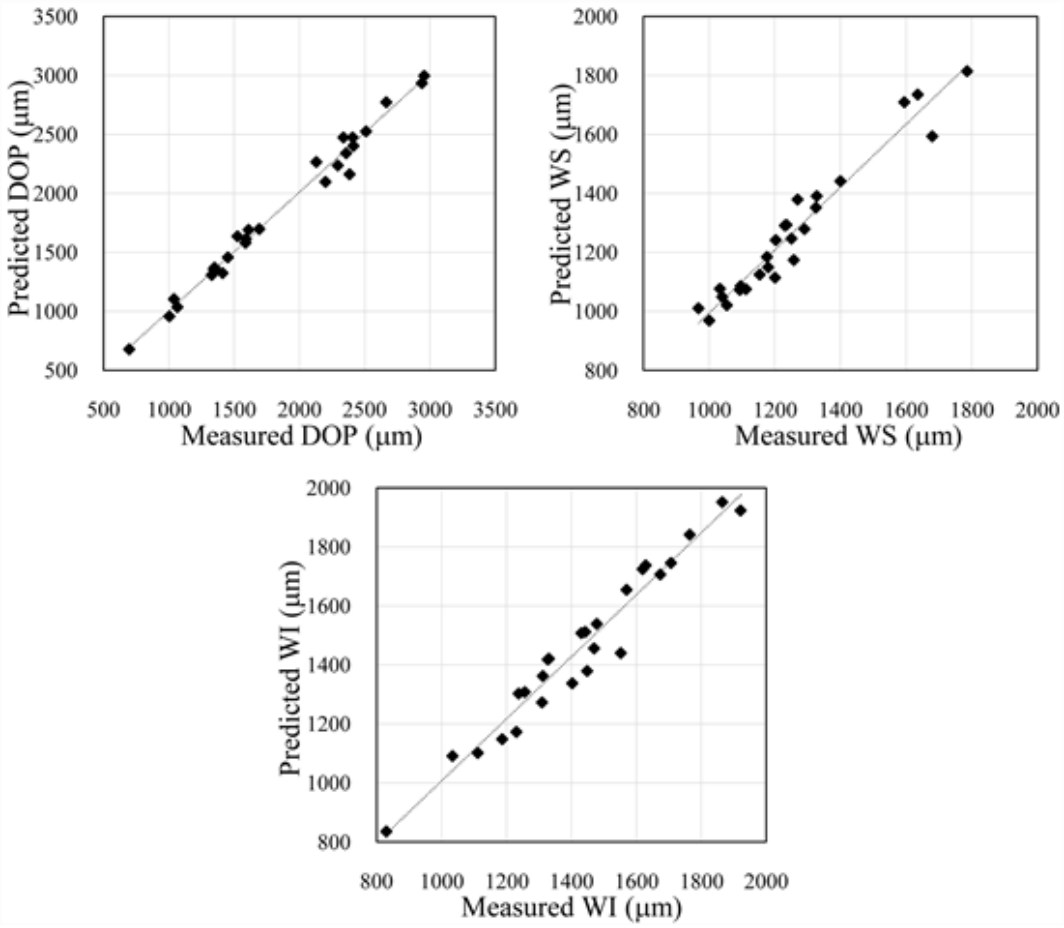

Figure 12 : Measured and predicted weld dimensions.

1.6 CONCLUSION

This paper presents an experimental investigation of laser overlap welding of low carbon galvanized steel. The experimental work is focused on depth of penetration, bead width at the surface, and bead width at the interface and hardness using various laser welding parameters such as laser power, welding speed, laser fiber diameter, and gap between sheets and sheet thickness. There are 27 experimental tests taken as all factors known to have an influence on welds quality to conduct a systematic study using an efficient and structured experimental design. An error of less than 10% achieved in repeatability tests ensures that the measurement results are consistent and robust. Based on these measurements and using various statistical analysis tools, the average effects of the laser welding parameters and the effects of their interactions on different weld geometrical characteristics variation are estimated and analyzed. Their contributions in weld quality variation are also evaluated. The micro hardness measurements show coherent results with an increase in the weld hardness from 150 Hv to 250 Hv. A multivariate analysis reveals that each weld geometrical attribute is correlated to a specific group of welding parameters. Explicit and quantified criteria are used to identify the most relevant variables for a consistent and practical predictive modeling. The welding parameters that have significant effects on the weld quality are laser power, welding speed and laser fiber diameter. The gap between sheets has a very limited effect. Confirmed by a multiple correlation analysis between weld geometrical attributes and welding parameters, the results suggest that many options can be considered for building an efficient weld quality prediction model. An artificial neural network based simplified predictive model is given as an example to demonstrate the possible and promising performance of weld quality prediction that can be achieved.

CHAPITRE 2
MODELE NUMERIQUE DE PREDICTION DES CARACTERISTIQUES GEOMETRIQUE DES SOUDURES OBTENUES DU SOUDAGE AU LASER PAR RECOUVREMENT DE L'ACIER GALVANISE FAIBLE TENEUR EN CARBONE

2.1 RÉSUMÉ EN FRANÇAIS DU DEUXIÈME ARTICLE

Le soudage au laser (SL) devient l'un des procédés d'assemblages les plus importants, de point de vue économique et qualitatif. SL permet un apport de chaleur bref et localisé, limitant les distorsions thermiques et favorisant l'assemblage des composants sensibles à la chaleur. L'exploitation efficace des avantages offerts par SL, requiert une stratégie qui permet d'identifier et de contrôler les variables du procédé de soudage pour produire des soudures avec les caractéristiques souhaitées sans recourir aux procédures classiques d'essais et d'erreurs. Cet article présente une étude de modélisation par éléments finis du soudage au laser par recouvrement de l'acier galvanisé à faible teneur en carbone. Son but est la prédiction des caractéristiques géométriques des cordons de soudure. L'approche de modélisation proposée est fondée sur les équations de transfert de chaleur et tient compte des propriétés du matériau dépendant de la température, des transformations métallurgiques et de l'enthalpie de changement de phase. Une source de chaleur 3D adaptative est utilisée pour simuler le faisceau laser à la fois en mode trou de serrure et en mode conduction. Le modèle 3D développé sur le logiciel commercial COMSOL, est utilisé pour estimer les caractéristiques géométriques du cordon de soudure pour divers paramètres sur une plage de variation suffisamment large, tels que la puissance laser, la vitesse de soudage et le diamètre du faisceau laser. Une série de données expérimentales obtenue à l'aide d'un laser Nd-YAG 3 kW, a servi à la validation du modèle numérique. Des outils d'analyse statistique confirmés sont utilisés pour évaluer la qualité de prédiction du modèle. Les résultats révèlent que

l'approche de modélisation peut fournir non seulement une prévision cohérente et précise des caractéristiques de la soudure dans des conditions de soudage variables, mais également une analyse complète et quantitative des effets des paramètres du processus sur la qualité de la soudure. Les résultats montrent une grande concordance entre les valeurs prévues et mesurées des attributs géométriques du cordon de soudure, notamment la profondeur de pénétration, la largeur du cordon à la surface supérieure et sa largeur à l'interface, avec une précision de prédiction supérieure à 95%.

Ce deuxième article, intitulé « *A Three-Dimensional Numerical Model for Predicting the Weld Bead Geometry Characteristics in Laser Overlap Welding of Low Carbon Galvanized Steel* », fut rédigé par moi-même ainsi que par le professeur Abderrazak El Ouafi. Il a été publié en 2019 dans la revue *Journal of Applied Mathematics and Physics*. En tant que premier auteur, ma contribution à ce travail fut l'essentiel de la recherche sur l'état de l'art, le développement de la méthode, l'exécution des tests de performance et la rédaction de l'article. Le professeur Abderrazak El Ouafi, second auteur, a fourni l'idée originale. Il a aidé à la recherche sur l'état de l'art, au développement de la méthode ainsi qu'à la révision de l'article.

2.2 ABSTRACT

Laser welding (LW) becomes one of the most economical high-quality joining processes. LW offers the advantage of very controlled heat input resulting in low distortion and the ability to weld heat sensitive components. To exploit efficiently the benefits presented by LW, it is necessary to develop an integrated approach to identify and control the welding process variables in order to produce the desired weld characteristics without being forced to use the traditional and fastidious trial and error procedures. The paper presents a study of weld bead geometry characteristics prediction for laser overlap welding of low carbon galvanized steel using 3D numerical modelling and experimental validation. The temperature dependent material properties, metallurgical transformations and enthalpy method constitute the foundation of the proposed modelling approach. An adaptive 3D heat source is adopted to simulate both keyhole and conduction mode of the LW process. The simulations are performed using 3D finite element model on commercial software. The model is used to estimate the weld bead geometry characteristics for various LW parameters, such as laser power, welding speed and laser beam diameter. The calibration and validation of the 3D numerical model are based on experimental data achieved using a 3 kW Nd-YAG continuous laser system, a structured experimental design and confirmed statistical analysis tools. The results reveal that the modelling approach can provide not only a consistent and accurate prediction of the weld characteristics under variable welding parameters and conditions but also a comprehensive and quantitative analysis of process parameters effects on the weld quality. The results show great concordance between predicted and measured values for weld bead geometry characteristics, such as depth of penetration, bead width at the top surface and bead width at the interface between sheets, with an average accuracy greater than 95%.

2.3 INTRODUCTION

The reduction of energy consumption and atmospheric pollution as well as the improvement of safety have led the automotive industry reconsider their design methods in order to decrease the weight of vehicles by using high performance materials. The tailored welded banks are now the major components constituting the new vehicle body. This design approach aims to optimize the weight of the vehicle structure by joining sheets from various nuances of high resistance material and different thicknesses. Therefore, the quantity of welds in the car body was more than doubled in the last years. In these conditions, the aptitude of the welds to resist to diverse solicitations remains the main concern of engineers. This aptitude is conditioned largely by the weld cross section geometry characteristics [30]. The identification of the laser parameter adjustments that lead to desired welds characteristics, without being forced to use the traditional and fastidious trial and error procedures, requires accurate and robustly predictive modelling approaches. The modeling of laser welding has evolved through several stages, starting with fundamental heat equations based simple analytical models to the most complex numerical models taking into account practically all physical phenomena involved in the welding process [43-48]. The modeling of the heat source is one of the key elements in the evolution of laser welding models. Various modeling investigations reveal strong and direct correlation between the resulted thermal field and adopted heat source model. The first heat source model for welding was proposed by Rosenthal in 1946 where the heat source was presented in the form of a point moving along a semi-infinite work piece [49]. This model can be applied to simulate the welding of thick parts and also for surface heat treatment by laser. Using Rosenthal solution, Friedman developed in 1975, a modeling approach for estimating temperatures, stresses and distortions resulting from the welding process, using finite element method applied to butt joint welding [50]. Ashby and Easterling proposed a model where the heat source is simulated to a line source moving parallel to the surface. This model is extensively used in surface heating [51]. A double ellipsoid heat source developed by Goldak is used to simulate the deep-penetration welding [52] . This type of heat source model is used by several studies of arc welding, laser

welding and laser heat treatment[53-55]. In the majority of cases, Gaussian heat sources presented the best option especially for laser welding [56]. Gaussian rotary volumetric heat source model proposed to simulate the heat input of laser energy in a finite element thermal analysis of laser welding of galvanized high-strength steel in a zero-gap lap joint configuration produced good results for the weld pool size prediction [54]. Models using the same type of heat source provided better results in the temperature fields estimation compared to other types of heat sources [55]. More recently, the combination of two types of heat sources, such as Gaussian conical combined with cylindrical heat source is proposed [57]. Nail head heat source resulting from the combination of point and line sources is used to describe the keyhole formation [43]. Wang proposed another model using a polynomial heat source for welding based on a Gaussian heat density distribution, by combining disc source for surface heating and polynomial equation for volumetric penetration [44]. Chande and Mazumder also investigated moving Gaussian heat source in a 3D laser welding modeling using finite differences numerical technique [45]. Despite the relatively good results obtained, the models performance remains quite limited. The advent of finite element computing software offered the possibility to build multi-physics and complex models integrating diverse interacting phenomena in the welding process. This permitted the development of many useful models to understand the evolution of welds formation and to identify the effects of this evolution on the quality of the resulting welds. As examples, the thermo-hydraulic 2D models developed to simulate the keyhole formation including the melting and vaporization of the metal [46] or to understand the evolution of the liquid/gas interface during pulsed laser welding [47]. Another study reported that convection heat transfer plays a very important role in the welding process and considered the most important factor influencing the shape and the geometry of the weld cross-section [57]. It is also reported in this study that convection heat transfer may be responsible for certain defects, such as variable penetration and lack of fusion. A hydrodynamic laser welding model including the effect of recoil pressure on the flow of molten metal is proposed reveal that the convective heat transfer induced by the recoil pressure is important for the laser absorption [58]. Chan investigated the flow in a molten pool generated by the laser by taking into

account the convection of Marangoni [59]. The Marangoni phenomenon modifies the characteristics of the melting and solidification process and makes the melt wider and shallower. The thermal properties of the material are also significant factors in the formation and shape of the melting pool [60]. The prediction of the mechanical characteristics of the welds does not always require complex models. In a detailed literature review, Mackwood and Crafer indicated that the thermal models are often sufficient and efficient in the case of laser welding [50]. However, in most studies, the heat sources are used in keyhole mode and conduction mode separately, and in most cases, the models are applied on laser welding in butt joint configuration. Oussaid et al. conducted an experimental investigation to evaluate the effects of various laser welding parameters on the welding quality [20]. Laser power, welding speed, laser fiber diameter, gap between sheets and sheets thickness are combined and used to evaluate the variation of three geometrical characteristics of the weld: penetration depth, bead width at the surface and bead width at the interface. In this study, various improved statistical tools are used to investigate the effects of the welding parameters on the weld quality and to identify the possible relationship between these parameters and the geometrical characteristics of the weld. The investigation results reveal that there are many options can be considered for building an efficient welds quality prediction model. Results achieved using an artificial neural network (ANN) based simplified model demonstrated promising model performances. Indeed, when a fast and efficient prediction model is needed, ANN offers many advantages especially in the case of computationally intensive predictions and real-time applications where numerical models are very slow and not adapted. ANN models have been used with success to model many welding processes. However, ANN model can accurately predict the weld geometry as well as the change in weld pool profiles like between conduction mode and keyhole mode only if trained with good and appropriate data. Moreover, producing an accurate and flexible ANN model requires very large data to ensure efficient ANN learning and validation processes. On the other hand, the generation of the needed data using experiment is relatively long and expensive. Therefore, experimentally validated 3D finite element method-based models can be used to generate acceptable and cost-effective data. The present paper describes the development of a 3D numerical model to

be used for generating the additional data needed to build the most accurate, flexible and efficient ANN based model for predicting the weld bead geometry characteristics in laser overlap welding of low carbon galvanized steel. An integrated approach combining 3D numerical modeling and experimental validation is proposed to produce the most consistent predictions. The welding process simulation is carried out by 3D finite element model using COMSOL Multiphysics software. The numerical modelling is built on simple heat transfer model based on a moving heat source in a finite medium volume to evaluate the temperature field, and thus to estimate the melting zone dimensions and the weld geometry characteristics for various welding parameters and conditions. The model is based on an improved adaptive 3D heat source used to simulate both key-hole and conduction laser welding process mode. The volumetric heat source is calibrated using specific factors defined as function of the laser parameters to adapt respectively the weld bead width and the absorption depth of the laser beam. The latent heat of fusion is taken into account by adapting the material temperature dependent specific heat in the temperature range situated between solidus and liquidus. The calibration and validation of the model are achieved using experimental data produced on a commercial 3 kW Nd-YAG laser system performed according to a structured experimental design and confirmed statistical analysis tools. The results reveal that the 3D numerical model is able to provide not only a consistent and accurate prediction of the weld bead geometry characteristics under variable welding parameters and conditions but also a comprehensive analysis of the average effects of the welding parameters on the weld quality. The results show great concordance between predicted and measured values of the weld characteristics. The paper is organized in four parts as follows. The first presents an introduction, a brief review and the objectives of the study. The second outlines succinctly the numerical method, describes the model, the governing equations and the simulation parameters and conditions. The third discusses the numerical and experimental results. The fourth presents the conclusion of the work and outline the potential direction of future research.

2.4 METHOD AND MATERIALS

2.4.1 Model Description

The 3D simulation model of the laser welding process in overlap joint configuration consists to irradiate two overlapped low carbon galvanized steel sheets with respective thickness of 1 and 2 mm, as presented in **Figure 13**. The laser beam directed to the upper surface moves along a straight line, which becomes the axis of the performed weld bead. The laser beam is represented as a moving 3D volumetric heat source with a conical Gaussian distribution so that the integral of the air under the heat distribution curve equals to a unit as illustrated in **Figure 14**.

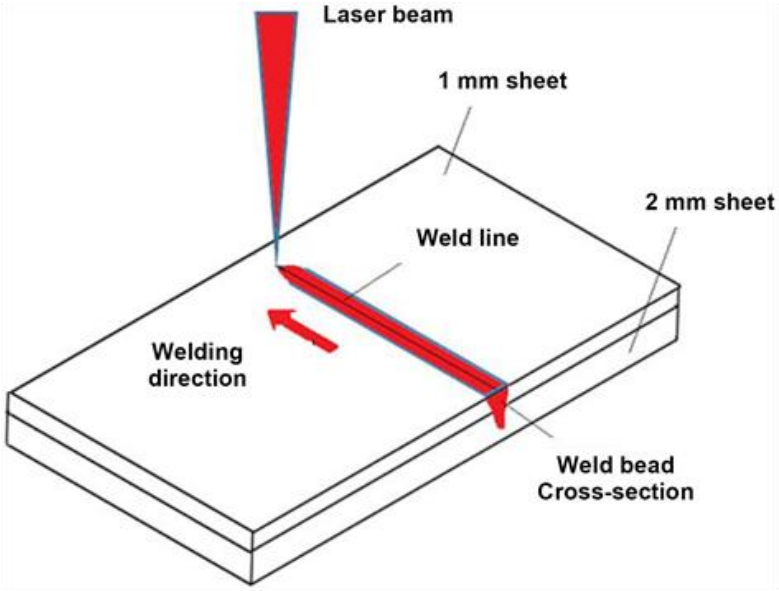

Figure 13: Overlap laser welding model description

The heat source model expressed as function of the laser welding parameters and the material properties is used to determine the size and the shape of the weld cross section. This

representation allows to evaluate the weld bead geometry characteristics variation as function of the laser welding parameters [49]. The proposed model is however built under various simplifying assumptions such as: 1) the influence of zinc vapor diffusion on the thermal properties of weld zone is ignored. 2) The experimental investigations revealed a relatively limited effect of the gap size on different weld geometric characteristics. The maximum observed contribution of the gap in these characteristics' variation represents approximately 5%. Therefore, the gap size is not considered as variable in the present model. 3) The material is considered homogeneous and isotropic. 4) The welded parts are considered free from any geometrical imperfection, and finally 5) Fluid flows, Marangoni effect and the latent heat of vaporization are not considered in order to simplify the model and to avoid long simulations.

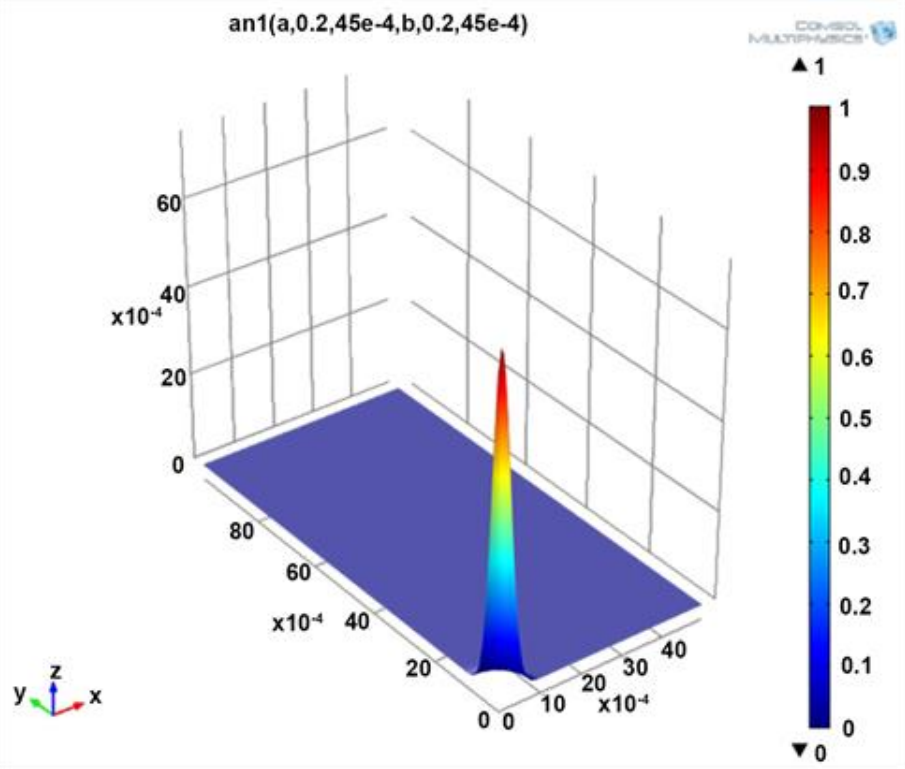

Figure 14: Gaussian distribution of laser beam power

2.4.2 Heat Transfer Formulation

The proposed model is based on conduction heat transfer including melting phase change. Equation (1) called Fourier's second law, describes the transient heat conduction in the solid. Solving this well-known equation permit to obtain the temperature field distribution in welded sheets at specific time and spatial coordinates.

$$\rho C_P \frac{\mathrm{d}T}{\mathrm{d}t} = k\nabla^2 T + Q(x, y, z, t) \qquad (1)$$

where ρ, k, C_P and Q Denote respectively the material density, the thermal conductivity, heat capacity and the heating power per unit volume.

The melting phase change is included into the model both in term of latent heat of fusion and the temperature dependant properties. The enthalpy method is used to model the phase transition by modifying the temperature dependent heat capacity as denoted in Equation (2) and illustrated in **Figure 15** [47].

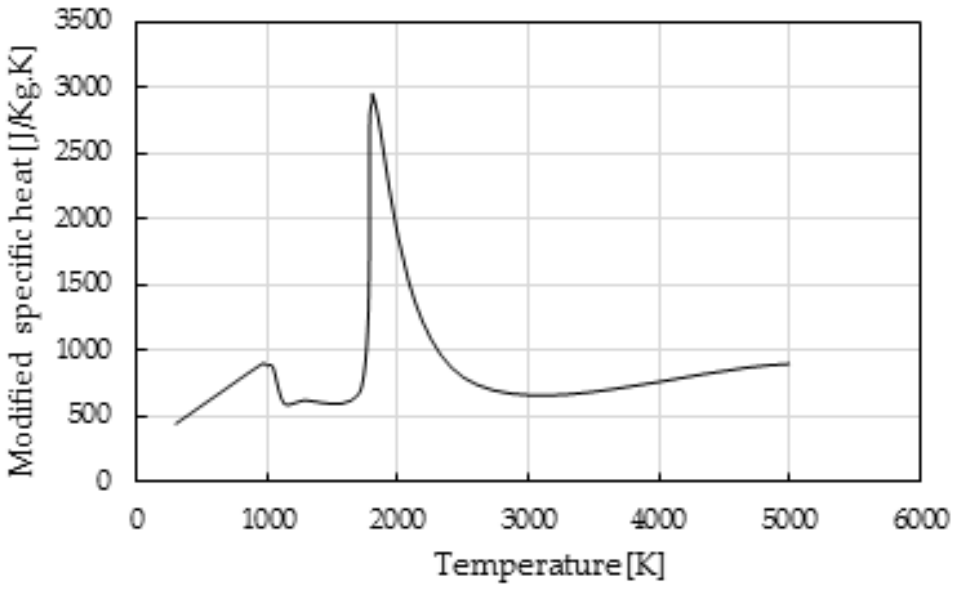

Figure 15 : Temperature dependent specific heat including the enthalpy of fusion.

$$C_P = C_P^*(T) + \frac{1}{\Delta T\sqrt{\pi}} e^{-\frac{T-T_f}{\Delta T^2}} L_f \quad (2)$$

With T_f the melting point, L_f the latent heat of fusion and ΔT a temperature range of solid/liquid phase change set to 72K.

2.4.3 Boundary and Initial Conditions

At the initial time, sheets temperature is uniform and set at the room temperature *T_0=295 K*. Heat exchange between the welded parts and their external environment is integrated into the numerical model as a heat loss, which is expressed by convection and radiation. The convection occurs in the top surface and frontal surfaces. The convection is expressed as :

$$Q_{conv} = h(T - T_0) \quad (3)$$

With *h* the natural convection coefficient and T_0 the room temperature.

The radiation is occurred at the top surface and expressed by the Boltzmann law:

$$Q_{rad} = \sigma\varepsilon(T^4 - T_0^4) \quad (4)$$

With $\boldsymbol{\sigma}$ Boltzmann constant and $\boldsymbol{\varepsilon}$ the material emissivity.

The bottom surface is supposed thermally insulated according to the following equation:

$$-n(k\nabla T) = 0 \quad (5)$$

Since the geometry and laser beam are symmetric across the y-axis, the symmetry boundary condition suggests that only half of the geometry is modeled. This symmetry simplification ignores the laser beam misalignment during welding and the geometrical

imperfections of the parts. The symmetry simplification has drastically reduced the computational time. **Figure 16** is a representation of the thermal transfers and boundary conditions applied to the welded sheets.

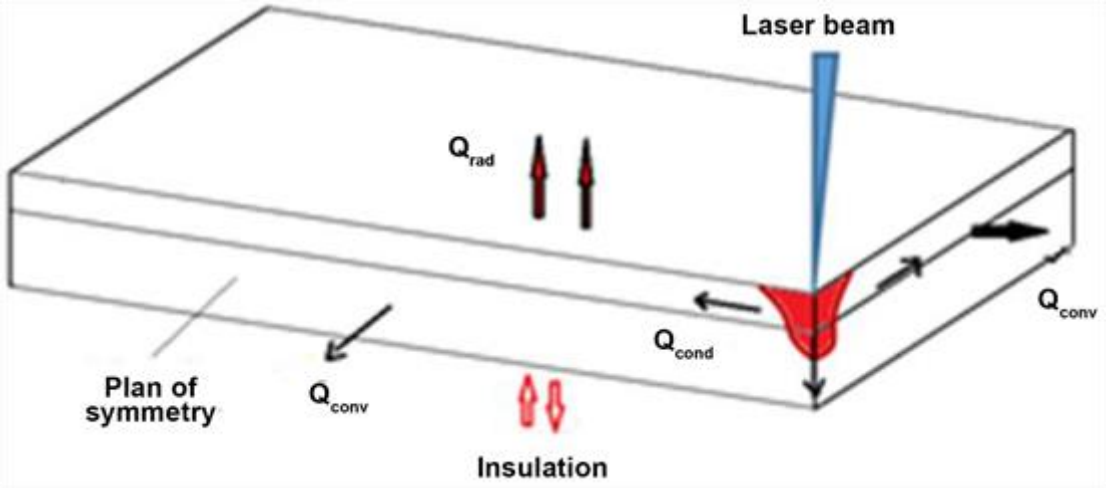

Figure 16 : Heat transfer modes and boundary conditions applied to the laser welding process.

2.4.4 Heat Source Modeling

The identification of adequate heat source is the most important step in welding process model building. According to the literature, a conical heat source with Gaussian distribution is the simplest and the most appropriate for predicting the shape of the laser weld bead cross-section [61]. Depending on the density of laser energy and the interaction time with the metal parts, two welding modes are possible: the conduction mode and the keyhole mode. The conduction mode occurs before reaching the vaporization temperature of the metal. In this mode, the energy is absorbed directly by the metal and dissipated by conduction in all directions, thus favouring round and wide welds with small penetration. In keyhole mode, which is characterized by a high energy density and a sufficiently slow interaction time, the irradiated surface of the metal reaches rapidly the vaporization temperature. These

vapours create an evacuation channel, which allows a better and deeper absorption of the laser beam energy, thus producing deep and sharp v-welds [12].

In General, to differentiate between the two welding modes during modeling simply assign a heat source to each mode. A 2D surface heat source (Equation (6)) to the conduction mode and a 3D volumetric heat source (Equation (7)) to the keyhole mode. The transition between the two modes must take place at the vaporisation temperature, but this increases the model complexity, because it can happen, for the same laser conditions, to start the simulation with 2D heat source and finish with 3D heat source.

$$Q(x,y,t) = \frac{Q_0 A(1-R)}{2\pi r^2} \cdot exp\left(-\frac{(x-x_0)^2}{2r^2} - \frac{(y-vt)^2}{2r^2}\right) \quad (6)$$

$$Q(x,y,z,t) = \frac{Q_0 A(1-R)}{2\pi r^2} \cdot exp\left(-\frac{(x-x_0)^2}{2r^2} - \frac{(y-vt)^2}{2r^2} - A_c|z|\right) \quad (7)$$

Since the difficulty to set the transition threshold according to laser parameters, an adaptive 3D heat source, moving in the y axis direction, is used to simulate both keyhole and conduction mode (Equation (8)). This volumetric heat source is calibrated by introducing two coefficients (m and n) to adapt respectively the weld bead width and the absorption depth of the laser beam. These coefficients are related to the laser parameters with the most significant contribution to the variation of weld characteristics [62].

$$Q(x,y,z,t) = \frac{Q_0 A(1-R)}{2\pi r^2} exp\left(-\frac{(x-x_0)^2}{(mr)^2} - \frac{(y-vt)^2}{2r^2} - nA_c|z|\right) \quad (8)$$

Where Q_0, v, A, R and r denote respectively laser power, welding speed, material absorptivity, material reflectivity and laser beam radius.

The coefficients *m* and *n* are estimated as function of the laser parameters using the following empirical relationships:

$$m = 1.194\ -173\ 10^{-6}\ Q0[W] + 18.33\ v\left[\frac{m}{s}\right] + 649\ d[m] \quad (9)$$

$$n = 0.565 - 83\ 10^{-6}\ Q0[W] + 9.44\ \left[\frac{m}{s}\right] + 123\ d[m] \quad (10)$$

2.4.5 Geometry and Material Properties

The geometry is discretized using an extremely refined tetrahedral mesh at the neighborhood of the weld line and large mesh elements in the rest of the geometry. A mesh convergence study is conducted to determine the optimal mesh size, by simulating the welding process using the same laser parameters setting (2500 [W] laser power, 55 [mm/s] welding speed and 395 [μm] laser beam diameter) and different mesh sizes around the weld line.

As illustrated in **Figure 17**, the temperature is evaluated at a specific time in two points, located respectively in the top surface and the interface of the melting pool, according to different mesh sizes. Convergence curves show that temperatures become unchanged for mesh value less than 0.15 mm, otherwise, temperatures fluctuate due to errors in accuracy and truncation. To reduce the calculation time, the width and length of the geometry are reduced, on condition that the weld attributes are evaluated in the area where the welding process has reached its stationary state. The final dimensions of the meshed geometry are illustrated in **Figure 18**.

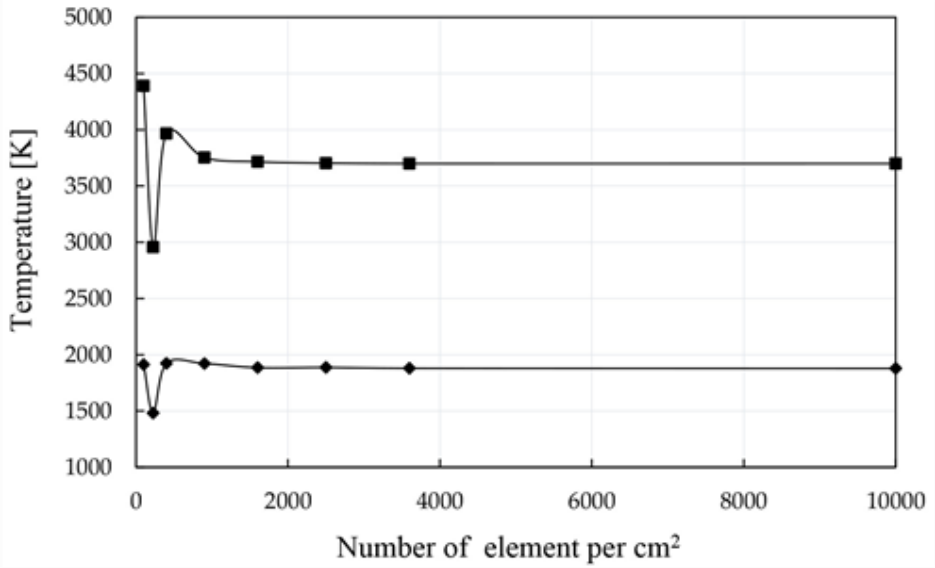

Figure 17 : Mesh convergence study.

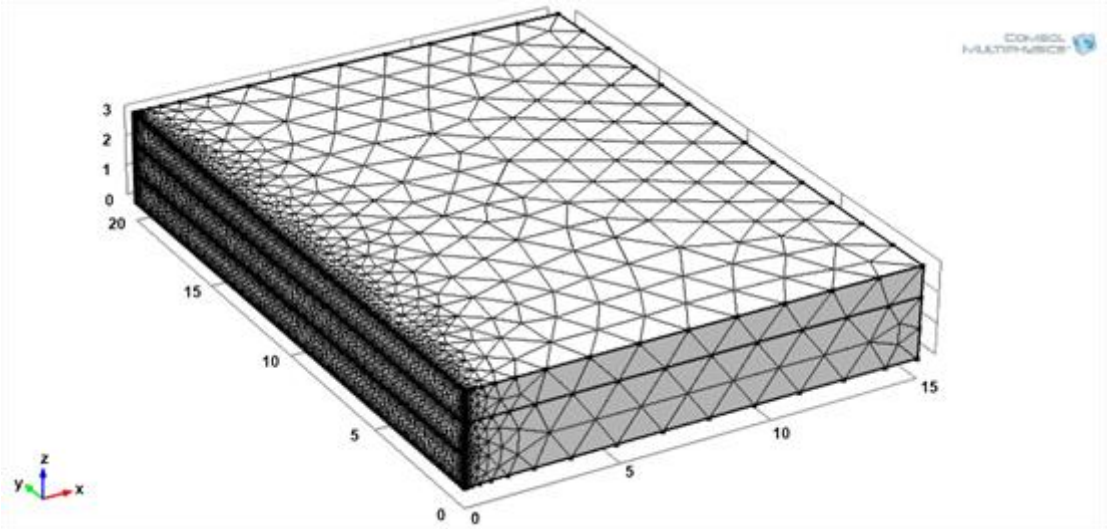

Figure 18 : Finite element mesh of weld specimen.

In order to validate the proposed model, typical ASTM A635 CS galvanized steel sheets with A40 coating type commonly used in the automotive industry are used to perform the overlap joint welds. The temperature dependant properties of this low carbon steel, which are density, thermal conductivity and specific heat, integrated in model are summarized in **Table 9**. The material constants are presented in **Table 8**.

Table 8: Constant properties of low carbon steel

Property	**Symbol**	**Value**	**Unit**
Temperature liquidus	T_L	1806	K
Temperature solidus	T_S	1734	K
Latent heat of fusion	L_f	244	kJ/kg
Material emissivity	ε	0.6	-
Material Absorptivity	A	800	1/m
Material reflectivity	R	0.3	-

Table 9: Temperature dependent properties of low carbon steel.

Temperature [K]	**Density [kg/m^3]**	**Specific heat [J/(kg.K)]**	**Thermal conductivity [W/ (m.K)]**
298	7863	446	74.7
962	7639	903	35.7
996	7648	886	34.1
1039	7647	882	32.2
1126	7661	600	28.3
1273	7587	623	29.6
1723	7317	729	33.6
1785	7287	738	34.2
1804	7132	785	34.8
1806	7030	817	35
2503	6449	795	35

2.4.6 Laser Parameter Setting and Model Validation

A series of simulations and tests of validation were carried out simultaneously according to comprehensive and structured experimental design. As indicated in **Table 10** three levels are selected for each of the three laser parameters (laser power, welding speed

and laser beam diameter). These parameters and levels are fixed following a series of preliminary tests [62].

Both for simulations and experiments, the weld cross section dimensions are measured in the stationary state zone to evaluate three weld geometry characteristics: depth of penetration (DOP), bead width at the top surface (WS) and bead width at the interface between sheets (WI). The cutting plane is located in the middle of the work piece and simulation results are evaluated at time $t = L/2v$.

The total computation time depends on the welding speed: $time\_end = L/v$, while the time step depends on the laser beam diameter, such the position of the laser beam at time t_i is located at a distance $s = 2/3\ d$ from its previous position, ie at time $t\_(i-1)$. Where L is the model geometry length, d the laser beam diameter and v the welding speed.

Table 8 : Welding process parameters

Laser parameters	Symbol	Unit	Level 1	Level 2	Level 3
Power	Q_0	W	2000	2500	3000
Speed	v	mm/s	40	55	70
Diameter	d	Mm	300	395	490

2.5 RESULTS AND DISCUSSIONS

The contours of the weld cross sections are determined from the temperature fields based on the location of points reaching the liquidus temperature. The weld penetration depth and the weld seam width, respectively at the surface and at the interface are measured on the

cross sections of the weld using an adapted MATLAB indexing algorithm. **Figure 19** and **Figure 20** show examples of typical simulation and experimental results.

The predicted bead characteristics are then compared to the measurements obtained from the experiments. The model performance is evaluated using various statistical criteria estimating the prediction errors.

A number of methods are available to evaluate the model's performance by estimating the prediction errors. It is generally recommended to use several criteria to obtain a satisfactory prediction error estimate. The following four traditional estimates from forecasting techniques are often used: 1) the coefficient of determination (R^2), 2) the Mean Absolute Error (MAE), 3) the Mean Absolute Percent Error (MAPE), 4) the Mean Root Squared Error (MRSE), and 5) the Relative Mean Root Squared Error (RMRSE). They can be defined mathematically as :

$$R^2 = 1 - \frac{\sum_{i=1}^{n}(y_i - \hat{y}_i)^2}{\sum_{i=1}^{n}(y_i - \bar{y})^2} \tag{11}$$

$$MAE = \frac{1}{n}\sum_{i=1}^{n}|y_i - \hat{y}_i| \tag{12}$$

$$MAPE = \left(\frac{1}{n}\sum_{i=1}^{n}\left|\frac{y_i - \hat{y}_i}{y_i}\right|\right)100\ (\%) \tag{13}$$

$$MRSE = \frac{1}{n}\sqrt{\sum_{i=1}^{n}(y_i - \hat{y}_i)^2} \tag{14}$$

$$RMRSE = \frac{MRSE}{\bar{y}}100\ (\%) \tag{15}$$

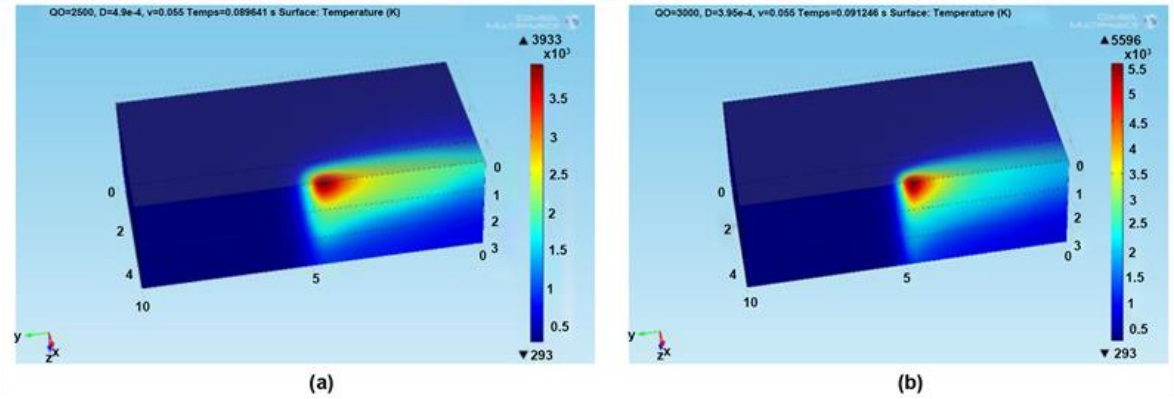

Figure 19 : Simulation results for a) P = 2500 W, V = 55 mm/s and D = 490 μm, and b) P = 3000 W, V = 55 mm/s and d = 395 μm.

Figure 20: Typical cross section shape of overlap welded galvanized sheets

Another dimension of the model evaluation consists to compare the laser parameters effects on the weld bead geometry characteristics extracted from ANOVA performed on the L9 experimental data with those extracted from ANOVA performed on simulation data. The combination of these statistical tools provides a very clear picture of the model performance by providing a satisfactory prediction error estimate. The performance of the model, based

on the selected five criteria, is presented at **Table 11**. The results reveal a good agreement between predicted and measured bead geometry characteristics. The model provides an R^2 more than 90% for the three weld characteristics. R^2 reaches 96%. The maximum observed MAPE remains less than 7.5% representing about 7%, 2.5% and 7.5 for DOP, WS and WI respectively. The maximum observed RMRSE remains less than 3.5% representing 3.04%, 1.09% and 3.32 for DOP, WS and WI respectively. The best model performance is obtained for WS with prediction errors 3 times lower than for DOP and WI. The highest errors are obtained for WI. This is explained by slight variation of the gap during the experiments. Globally, with such good results, the model is considered adequate to be used without difficulty in predictive strategies. The simulation data are generated from a structured L27 factorial design using the same parameter as in the experimentation. The choice of L27 is motivated by the possibility to evaluate the effect of the laser parameters interaction on the variation of weld bead geometry characteristics. The interaction cannot be evaluated by a fractional design.

Table 9 : Performance of the prediction of weld geometry characteristics.

	R2	**MAE**	**MAPE**	**MRSE**	**RMRSE**
DOP	90.94%	146.33	6.94%	60.22	3.04%
WS	96.09%	30.56	2.44%	13.84	1.09%
WI	94.12%	102.11	7.28%	40.75	3.32%

Table 12 summarises the ANOVA results based on the simulation data. The laser parameters effects, in term of percentage contributions of the (% C), on the variation of the three weld characteristics are practically the same as in the case of the experimental data. **Figure 21**, **Figure 22** and **Figure 23** illustrate the comparison of the % C obtained respectively from an L9 experimental data, an L9 simulation data and an L27 simulation data. These graphs reveal small differences between the three designs. The largest difference (less

than 10%) is observed for the power contribution in WI variation. This is probably due to the fact of not considering the gap in the simulations.

Table 10: Simplified ANOVA results for DOP, WS and WI

Source	DF	DOP		WS		WI	
		% C	F-Value	% C	F-value	% C	F-Value
P	2	28.53	960.01	47.03	796.22	28.24	82.13
D	2	12.61	424.09	10	169.25	22.23	71.45
V	2	56.14	1888.73	40.91	692.63	45.18	145.23
P*D	4	0.13	2.23	0.28	2.41	1.50	2.42
P*V	4	2.33	39.24	1.34	11.32	0.48	0.78
V*D	4	0.14	2.3	0.21	1.76	3.83	0.28
Error	18	0.12		0.24		1.24	
Total	26	100		100		100	

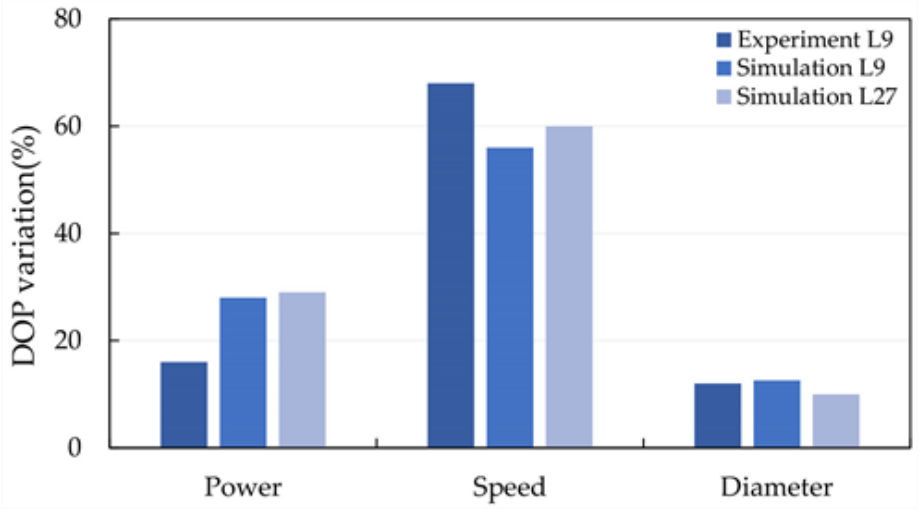

Figure 21 : Laser parameters contribution to the variation of DOP

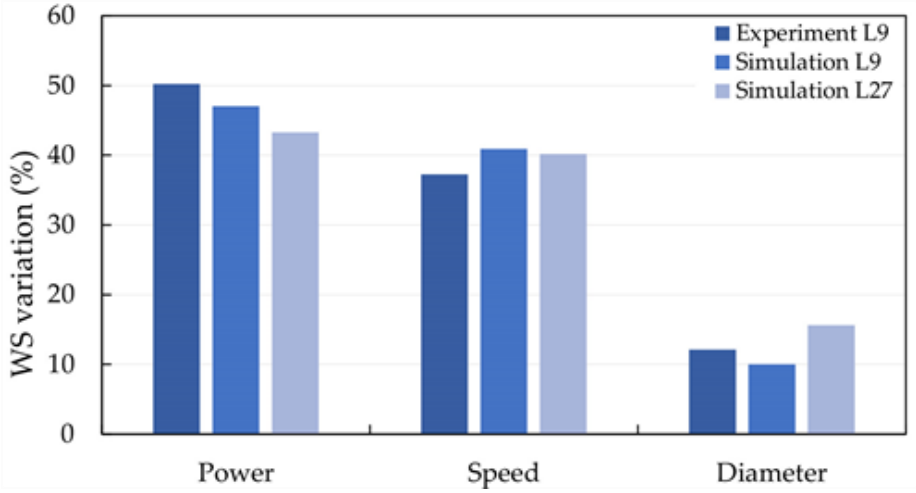

Figure 22 : Laser parameters contribution to the variation of WS.

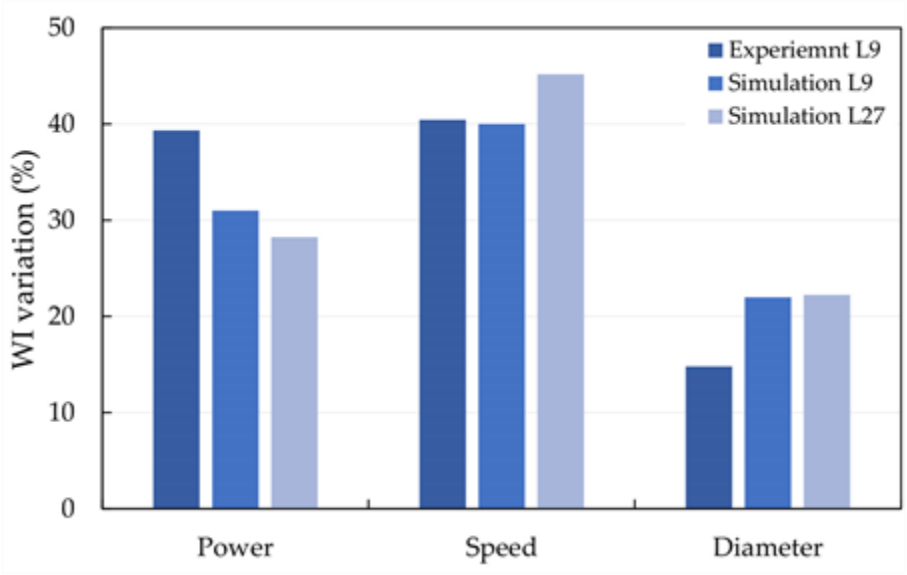

Figure 23: Laser parameters contribution to the variation of WS.

As established following the experimentation phase, the welding speed and the laser power are the most influential factors on the weld bead geometric characteristics, while the laser beam diameter effect remains relatively limited. The evaluation of the laser parameters interaction shows also non-significant effects. The total contribution of all interactions does not exceed 6%. It represents 2.6%, 1.83% and 5.81 for DOP, WS and WI respectively. These results are validated by the graphs of effects of the laser parameters on the weld bead

geometry characteristics presented in **Figure 24** An F-test is conducted to confirm the laser parameters contributions and effects-based conclusions.

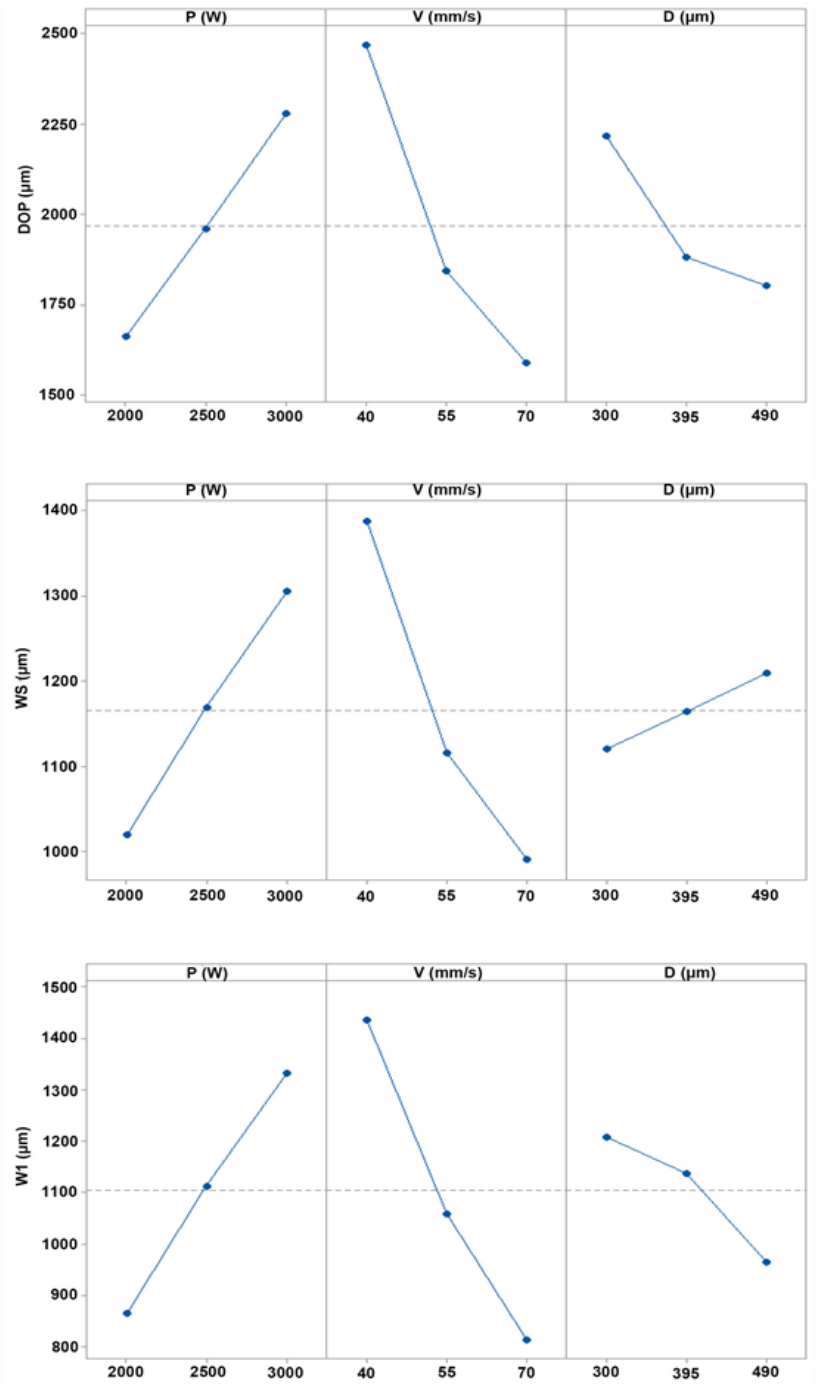

Figure 24 : Effects of laser parameters on weld characteristics variation

2.6 CONCLUSIONS

The present paper presents an integrated approach for building a forecasting 3D finite element model able to predict weld bead geometry characteristics for laser welding of low carbon galvanized steel in overlap configurations. An improved adaptive 3D heat source is used for simulating both keyhole and conduction mode. The implementation of the model is supported by a heat source calibration technique using specific modelling factors defined as function of the laser parameters to adapt respectively the weld bead width and the absorption depth of the laser beam.

A commercial 3 kW Nd-:YAG laser system, a structured experimental design and improved statistical analysis tools are used to evaluate the modelling approach and to confirm the prediction model accuracy. Extensively numerical simulations carried out through 3D finite element method reveal great concordance between modelling and experimental results. The comparison of predicted and measured weld geometric characteristics reveals an average accuracy greater than 95%. The prediction errors originate principally from experimental errors as well as from the considered assumptions. Globally, the results demonstrate that the numerical simulation can effectively lead to a consistent and accurate weld bead geometry characteristics prediction model under variable welding parameters and conditions and provide an appropriate framework for comprehensively qualitative and quantitative analysis of the effects of welding process parameters on the weld quality.

With the encouraging results obtained using this model, the laser overlap welding of low carbon galvanized steel will be the subject of additional and intensive investigations to generate more simulation and experimental data in order to develop an efficient ANN predictive modelling approach.

CHAPITRE 3
ÉTUDE SUR LA PRÉDICTION DE LA GÉOMÉTRIE DE LA SOUDURE AU LASER PAR RECOUVREMENT DE L'ACIER GALVANISÉ À FAIBLE TENEUR EN CARBONE BASÉE SUR LES RÉSEAUX DE NEURONES

3.1 RÉSUMÉ EN FRANÇAIS DU TROISIÈME ARTICLE

La modélisation prédictive pour l'analyse qualitative du procédé de soudage au laser devient une exigence critique pour assurer la fiabilité, l'efficacité et la sécurité du processus. Un modèle précis et efficace permettant d'effectuer une estimation de qualité d'une façon non destructive est un élément essentiel de cette évaluation. Cet article présente une approche structurée développée pour concevoir un modèle efficace basé sur les réseaux de neurones artificiels pour prédire les caractéristiques dimensionnelles des cordons de soudure obtenus du soudage au laser par recouvrement d'un acier galvanisé à faible teneur en carbone. L'approche de modélisation est basée sur l'analyse des effets directs des paramètres de soudage (puissance, vitesse de soudage, diamètre focal et gap) et ceux de leurs interactions sur les caractéristiques dimensionnelles du cordon de la soudure (profondeur de pénétration, largeur à la surface supérieure et la largeur à l'interface). Les données utilisées dans cette analyse proviennent d'une part, des investigations expérimentales structurées selon la méthode Taguchi et d'autre part des efforts exhaustifs de modélisation et de simulation 3D basées sur la méthode des éléments finis. En utilisant une conception factorielle, différents modèles de prédiction basés sur un réseau neuronal ont été développés, mis en œuvre et évalués. Les modèles ont été formés et testés à l'aide de données expérimentales, soutenues par les données générées par la simulation 3D. Des tests de validation combinés à divers

outils statistiques ont été utilisés pour évaluer l'influence des paramètres de soudage au laser sur les performances des modèles. Les résultats ont démontré que l'approche proposée a abouti à un modèle cohérent fournissant des prédictions précises et fiables des caractéristiques dimensionnelles du cordon de soudure dans des conditions de soudage variables. Le meilleur modèle présente des erreurs de prédiction inférieures à 7% pour les trois caractéristiques de qualité de la soudure.

Ce troisième article, intitulé « *A study on prediction of weld geometry in laser overlap welding of low carbon galvanized steel using ANN-based models* », fut rédigé par moi-même ainsi que par le professeur Abderrazak El Ouafi. Il a été publié en 2019 dans la revue Journal of Software Engineering and Applications. En tant que premier auteur, ma contribution à ce travail fut l'essentiel de la recherche sur l'état de l'art, le développement de la méthode, l'exécution des tests de performance et la rédaction de l'article. Le professeur Abderrazak El Ouafi, second auteur, a fourni l'idée originale. Il a aidé à la recherche sur l'état de l'art, au développement de la méthode ainsi qu'à la révision de l'article.

3.2 ABSTRACT

Predictive modelling for quality analysis becomes one of the most critical requirements for a continuous improvement of reliability, efficiency and safety of laser welding process. Accurate and effective model to perform non-destructive quality estimation is an essential part of this assessment. This paper presents a structured approach developed to design an effective artificial neural network-based model for predicting the weld bead dimensional characteristic in laser overlap welding of low carbon galvanized steel. The modelling approach is based on the analysis of direct and interaction effects of laser welding parameters such as laser power, welding speed, laser beam diameter and gap on weld bead dimensional characteristics such as depth of penetration, width at top surface and width at interface. The data used in this analysis was derived from structured experimental investigations according to Taguchi method and exhaustive FEM based 3D modelling and simulation efforts. Using a factorial design, different neural network-based prediction models were developed, implemented and evaluated. The models were trained and tested using experimental data, sup-ported with the data generated by the 3D simulation. Hold-out test and k-fold cross validation combined to various statistical tools were used to evaluate the influence of the laser welding parameters on the performances of the models. The results demonstrated that the proposed approach resulted successfully in a consistent model providing accurate and reliable predictions of weld bead dimensional characteristics under variable welding conditions. The best model present prediction errors lower than 7% for the three weld quality characteristics.

3.3 INTRODUCTION

Laser welding is an assembly process widely used in the industry, including the automotive industry. Overlap welding of galvanized steels enables joining of body car elements from different thicknesses. The disadvantage of the overlap configuration is the

premature vaporization of zinc, which generates pressure at the interface of the overlapped sheets. These pressurized vapors eventually eject the metal out of the melting pool or trapped as blowers after solidification.

Several experimental studies have shown the possibility of overcoming this situation by controlling the welding process parameters. Like the keyhole welding, which creates a channel permitting the evacuation of zinc vapors, an optimal gap between the parts to be welded also allows the lateral evacuation of these vapors. This means that a good control of welding parameters and conditions (laser power, welding speed, focal diameter, Gap between sheets and sheet thicknesses) can produce the desired welds characteristics.

Laser welding parameters play an important role in determining the mechanical characteristics of the weld seam [63]. Since the resistance of welded joints is linearly proportional to the shape and dimensions of the weld cross section, it is obvious to identify the relationship between the welding parameters and the geometrical attributes of the weld. To obtain welds with well-defined characteristics, the traditional test-failure method proves too expensive and more time-consuming. Finite element modeling has led to promising results through the performance of simulation software, but the complexity of the laser welding process, which includes many physical phenomena (thermal transfer, fluid flow, electromagnetic and thermodynamics), makes the models very complex; therefore, the calculation time becomes too long.

In contrast, thanks to their strong learning ability, artificial neural networks (ANNs) can establish nonlinear deterministic relationships between the inputs and the outputs of any system regardless of their complexity. ANNs are inspired by the human brain, they can learn and experience from examples, as they have a powerful ability to classify and recognize patterns. ANNs are used in many different fields of business, industry and science [64].

Synthia et al. [63] have developed a neural network-based prediction model of weld bead geometry according to laser welding parameters, in three different shielding gases (argon, helium and nitrogen). Another study applied an artificial neural network to predict a

geometry of GMAW welds with alternating shielding gases. The experimental results proved conformity and accordance with the predicted geometries. Furthermore, a sensitivity analysis showed that the welding speed is the most influential input parameter in the predicting model [65].

Frason et al. [66] developed a laser weld penetration monitoring system using an ANN to analyze acoustic emissions from the weld, and thereby determine the depth of penetration of the weld in real time. The system uses a fuzzy logic algorithm to compute the necessary speed changes to maintain the penetration at desired levels. An identical study used an ANN model to diagnose welding faults. Features extracted from the acoustic signals were used to train the ANN. After training, the ANN could identify normal and abnormal welds [67]. In the same vein, an ANN model uses data extracted from infrared thermal images that are recorded in real time during A-TIG welding, for the purpose of weld width and depth estimation [68]. Another study shows the possibility of using neural networks in the ascertainment of the weld quality for thermoplastics welded by laser transmission [69].

Olabi et al. [70] combined a backpropagation ANN with Taguchi design for experiments in order to optimize the parameters level (welding speed, laser power and focal position) of CO2 keyhole laser welding process in butt joint configurations. The laser welding of stainless steel in butt joint configuration was modeled using backpropagation trained neural network. The predicted weld dimensions showed conformance with the measured weld cross sections [29]. Casalino et al integrated an artificial neural network into the laser welding process, in order to optimize process parameters when welding stainless steel and increase its efficiency [71].

Depending on their architecture and their fields of application, several types of ANN exist. A broader description of different neural networks is presented in the literature review made by Zhang et al. [64]. The Multi-layer feedforward ANN are the most popular and widely used ANN in many applications, especially forecasting, because of their great ability to map nonlinear and complex relationships in multi-inputs multi-output context [28, 42, 72]. Jacques et al. proposed an ANN based predictive modelling approach for weld shape and

dimensions in butt joint laser welding of galvanized steel [73]. The resulting model presents excellent predictions with an average error less than 10%. This model, however, can only be applied in the case of laser welding in butt joint configurations.

Only a few studies used ANNs to predict the quality of laser welding of galvanized steels and even less in overlap configurations. The few attempts revealed in the literature are focussed on specific application of the ANNs without explicit and detailed references to the nature of the data used in the models training and validation and criteria adopted for the model performances evaluation. These fundamental ideas that constitute the basic ingredients of any models optimization procedure are indispensable to build an efficient predictive modeling approach.

The present paper presents an artificial neural network-based model for predicting the weld bead dimensional characteristic in laser overlap welding of low carbon galvanized steel. The modelling approach is based on laser welding parameters such as laser power, welding speed, laser beam diameter and the Gap between the overlapped parts to estimate specific weld bead dimensional characteristics such as depth of penetration, width at top surface and width at interface. A series of data provided from experiments using a 3KW Nd-YAG laser source in a well-structured Taguchi design are combined with simulation data provided by a 3D finite element model to train and test the ANN built using variables selection based factorial design. Hold-out test and k-fold cross validation combined to various improved statistical criteria are used for assessing the model's performance.

3.4 MODELING APPROACH

3.4.1 Methodology

The purpose of this study is to set up a model able to predict accurately and quickly three geometrical characteristics of the weld seams: depth of penetration (DOP), weld width

at the top surface (WS) and at the interface (WI) as defined in **Figure 4**. The three welds characteristics prediction in overlap laser welding configuration of low-carbon galvanized steel is based on laser power (P), welding speed (S), laser beam diameter (D) and Gap (Gap) between the overlapped sheets as variables. The prediction model is achieved using an artificial neural network-based model (ANN).

In order to know the most influential laser welding parameters on the model accuracy, as well as the effects of these parameters on the quality of the of weld characteristics prediction, 16 models are built according to a full factorial design including the variables known for their influence on the variation of the geometrical characteristics of the weld. As shown in **Table 13**, a variable takes the value 1 when it is included in the model and 0 when it is not.

To eliminate the maximum random error sources, the learning data inputs, and the testing data inputs must represent the same population, i.e. both should be contained in the same variation range. This is the case in the present study, as shown in **Table 14**. Three levels are assigned to each parameter. The upper and lower limits of factors are respectively 2000 to 3000 W for the power of the laser, 40 to 70 mm/s for the welding speed, 300 to 490 μm for the beam diameter and 0.05 to 0.15 mm for the Gap. The Data assigned for training and testing the various models are partly provided from an experimental investigation of laser welding process [62] while the other part is produced by a 3D FEM simulation [74]. In order to include the gap in the ANN modeling, the finite element model is adapted for each Gap value (0.05, 0.1 and 0.15 mm) by recalculating the calibration coefficients (m and n) of the heat source for each time step.

The database generated by simulations is structured in a full factorial design of 4 factors, each at three levels, while experimental data are planned in three L9 orthogonal matrix. For each gap value, to determine the true prediction errors of an ANN model and its accuracy for future predictions, new unused data in learning stage should be used in model testing phase, because learning errors are often inferior to validation errors. To do this, two

table 11: Input variables of each of the ANN models.

Model	Gap	Power	Speed	Diameter
M1	1	1	1	1
M2	0	1	1	1
M3	1	0	1	1
M4	1	1	0	1
M5	1	1	1	0
M6	0	0	1	1
M7	0	1	0	1
M8	0	1	1	0
M9	1	0	0	1
M10	1	0	1	0
M11	1	1	0	0
M12	1	0	0	0
M13	0	1	0	0
M14	0	0	1	0
M15	0	0	0	1
M16	0	0	0	0

Table 12: The selected levels for the process parameters

Level	Gap	Power	Speed	Diameter
1	0.05	2000	40	300
2	0.10	2500	55	395
3	0.15	3000	70	490

validation methods are adopted: «hold-out set method» and «k-fold cross validation method». The hold-out set method consists of using the large part of the data to train the model and the remaining data to test it. The k-fold cross validation method consists of sampling all the n data after its randomization in k segments, the model is then trained by n-k data and tested by k remaining data. The procedure is repeated k times by changing the testing sample each time. The validation errors are estimated by various statistical tools for the k variants, then averaged to determine the real prediction errors of the model.

The neural network modeling procedure used in this study consists first in confirming the reliability of the data provided by the 3D finite element model. Using the hold-out set method, the ANN models are trained by the entire simulation data and then tested by the experimental data. Second, all the data are mixed and randomized, then the k-fold cross validation method is applied, with k = 6.

3.4.2 ANN model building

There are several kinds of networks according to their architectures, their internal mechanisms and their application objectives. In the present study, the interest is focused on multilayer feedforward back propagation perceptron for its prediction capability. As

illustrated in **Figure 25**, the MLP is mainly composed of: (i) an input layer with a number of neurons equals the number of input variables of the ANN, called independent variables. (ii) One or more hidden layers having a limited number of neurons (n). It is necessary to try several networks for different values of n in order to optimize the training performances especially as the number of variables varies from one model to another and to avoid overtraining. Consequently, to avoid long training and overfitting that could affect the models accuracy, only one hidden layer is considered using n = 2 * p + 1, with p is the number of independent variables. (iii) An output layer containing a specific number of neurons equal to the number of output variables. In our case, there are three outputs (DOP, WS and WI).

The artificial neuron is an integrator that performs the weighted sum of its inputs originate from the previous layer (Eq. 16). The resulted sum is then transformed by a transfer function to provide the neuron output. The transfer function used for neurons of the input and hidden layer, is a sigmoid (Eq. 17), and that used for the output layer neurons is a linear function (Eq. 18).

$$a = f(s) = f(xW^T - b) \quad (16)$$

$$f(s) = 1/(1 + e^{-s}) \quad (17)$$

$$f(s) = s \quad (18)$$

Where x, w^T and b denote respectively neuron input, Wight matrix and bias.

The outputs of last layer neurons are then compared to the target values (dependent variables), if the difference is greater than the tolerated deviation, the network updates the weights associated to each neuron by means of a backpropagation technique and therefore starts a new computing loop, to help minimize the gap between the network output and the target value. Thus, the iterations continue until reaching a tolerated value of the error.

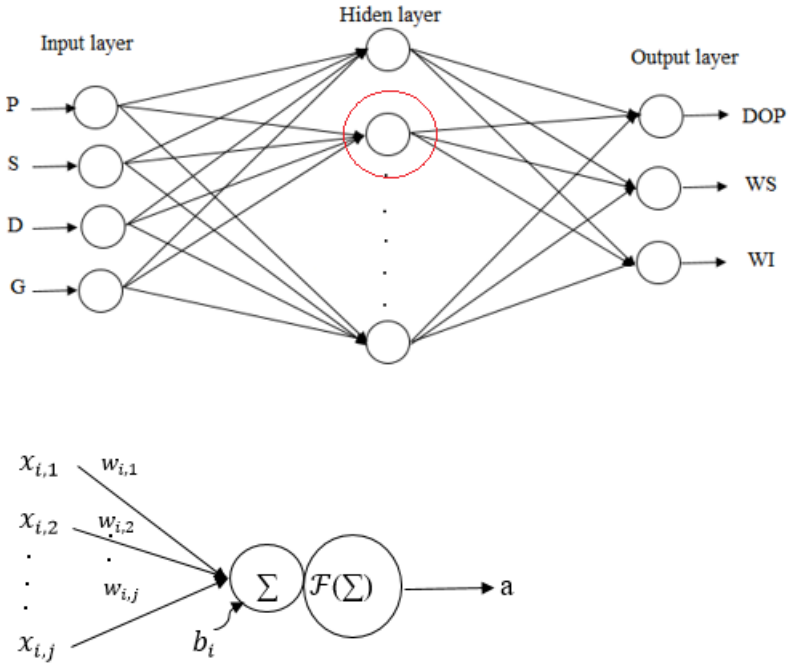

Figure 25 : Neural network architecture.

The networks are assembled using the built in MATLAB Netfiting Toolbox. The function used for the training of the various networks is the Levenberg-Marquardt function. This function uses an algorithm for supervised learning considered the fastest available algorithm by virtue of the validation vectors, which enables the network learning to stop prematurely if the performance in the validation matrix fails to reduce the error.

3.4.3 Model assessment

Based on the modeling process results, three statistical variables are estimated to evaluate the performance of each model: (i) Pearson Coefficient of determination R^2 which

is commonly applied to training errors. Its main defect is its growth with the addition of input variables to the model, whereas an excess of variables does not always lead to robust models. This is why one is interested in the Adjusted coefficient$\overline{R^2}$. (ii) Root mean squared error (RMSE) is the standard deviation of prediction errors (residuals), it measures the extent of these residuals and indicates the concentration of data around the line of best fit, and (iii) Mean absolute percentage error (MAPE) is a useful measure of forecasting accuracy. It is easy to interpret because it is expressed in percentage. The criteria are expressed mathematically as:

$$R^2 = 1 - \frac{\sum_{i=1}^{n}(y_i - \hat{y}_i)^2}{\sum_{i=1}^{n}(y_i - \bar{y})^2} \tag{4}$$

$$\overline{R^2} = 1 - \frac{(1 - R^2)(n-1)}{(n-p-1)} \tag{5}$$

$$MAPE = \left(\frac{1}{n}\sum_{i=1}^{n}\left|\frac{y_i - \hat{y}_i}{y_i}\right|\right)100\ (\%) \tag{6}$$

$$RMSE = \frac{1}{n}\sqrt{\sum_{i=1}^{n}(y_i - \hat{y}_i)^2} \tag{7}$$

Where $n, p, y_i, \hat{y}$ and $\bar{y}$ denote respectively sample size, number of input process parameter, actual output, predicted output and the mean actual output.

3.5 RESULTS AND DISCUSSIONS

The evaluation of the training and testing performances of the 16 models are based on the three statistical criteria applied to the two validation methods. First, the models training and testing performances using the hold-out set method are evaluated and the

contributions of the laser welding parameters to ANN model improvement are estimated. In this case, as the models are trained using numerical simulation data and tested by means of experimental data, the major part of the training errors are due to the laser welding parameters not considered as variables in the ANN model building and to the possible bias in the 3D numerical model predictions, while the observed testing errors are caused by experimental errors.

Table 15 illustrates the learning error estimates of the 16 ANN models using the three performance indicators mentioned above, namely RMSE, MAPE and $\overline{R^2}$. The comparison between the learning performances of the 16 models shows the contribution of the various welding parameters to the improvement of the model performances. The results show that the best model for the prediction of the three weld seam attributes (DOP, WS and WI) is indeed the model M_1, which contains the four process variables. The relative errors of DOP, WS and WI Prediction are 2.1%, 1.1% and 2.6% respectively. The M_2 model, which does not include the gap as input, also shows high performances in the prediction of the three weld seam attributes with respectively a relative error of 4.2%, 2% and 4.6%. In third place comes the M_5 model, which does not consider the focal diameter as input with prediction errors of 8.2%, 2.8% and 4.5% for DOP, WS and WI respectively. Among the two-variable models, the model M_8, which considers only the power and the welding speed as inputs, shows relatively good performance during learning stage. The DOP, WS and WI relative prediction errors are 8.9%, 3.2% and 6.1% respectively.

Variance analysis (ANOVA) results in **Table 16** and graphs of main effects presented in **Figure 26**, **27** and **28** are the two statistical tools used to evaluate the contribution of the laser parameters, as well as their interactions in the reduction of the prediction error estimator (RMSE) for the three geometric welding attributes (DOP, WS and WI).

Table 13: Training performance of the models using hold-out set method.

Model	DOP			WS			WI		
	RMSE	**MAPE**	$\overline{R^2}$	**RMSE**	**MAPE**	$\overline{R^2}$	**RMSE**	**MAPE**	$\overline{R^2}$
M1	68.9	2.1	1	20.2	1.1	1.01	53.5	2.6	0.99
M 2	142.3	4.2	0.95	35.5	2	0.97	80	4.6	0.89
M 3	263	9.3	0.79	119.3	7.1	0.50	179	10.4	0.53
M4	440.4	16.4	0.29	111.1	4.1	0.58	193	10.8	30.9
M5	237.9	8.2	0.82	47.8	2.8	0.93	79.8	4.5	0.89
M6	281.5	9.7	0.74	124	7.4	0.48	191	11.2	0.48
M7	449.2	16.2	0.27	107.6	6.2	50.8	196.8	11.4	0.36
M8	268.9	8.9	0.77	57.5	3.2	0.89	105.3	6.1	0.83
M9	476.2	16.9	0.16	147.6	8.4	0.17	238.9	13.3	0.064
M10	330.1	11.1	0.64	130.4	7.8	0.36	184.2	11	0.48
M11	476.7	17.0	0.16	117.7	6.8	0.50	191.3	11	0.375
M12	507.6	18.1	0.03	161	9.1	0.02	242.3	13.2	0.047
M13	487.1	17.2	0.12	121.8	7	0.47	204.6	11.8	0.32
M14	347.8	1.8	0.59	137.1	8.1	0.33	199	11.9	0.43
M15	486.1	17	0.12	151.7	8.5	0.15	250.9	14	0.018
M16	517.3	18.3	0	165.6	9.3	0	253.8	14.2	0

Despite their percentage differences, the graphs of effect reveal that all welding parameters have a positive effect on improving the prediction quality of the three geometric attributes of the weld. This asserts that the most accurate and reliable model is indeed the M_1 which considers all the variables.

Table 14: Contribution of laser welding parameters to the ANN models learning improvement

Source	RMSE_DOP			RMSE_WS			RMSE_WI		
	C %	F-Value	P-Value	C %	F-Value	P-Value	C %	F-Value	P-Value
Gap	0.51	5.18	0.057	0.29	5.22	0.06	1.18	20.46	0.003
P	8.28	84.63	0.000	54.4	988.6	0.00	41	711.54	0.000
S	77.5	792.4	0.000	34.4	624.5	0.00	50.1	868.69	0.000
D	6.42	65.6	0.000	2.70	48.9	0.00	0.43	7.43	0.030
P*S	3.25	3.25	0.001	7.34	133.3	0.00	6.18	107.2	0.000
P*D	0.72	7.34	0.030	0.10	1.89	0.21	0.18	3.21	0.116
S*D	2.05	20.98	0.003	0.17	3.08	0.12	0.34	5.84	0.046
P*S*D	0.53	5.42	0.053	0.23	4.2	0.08	0.17	3	0.127
Error	0.69	-	-	0.39	-	-	0.40	-	-
Total	100	-	-	100	-	-	100	-	-

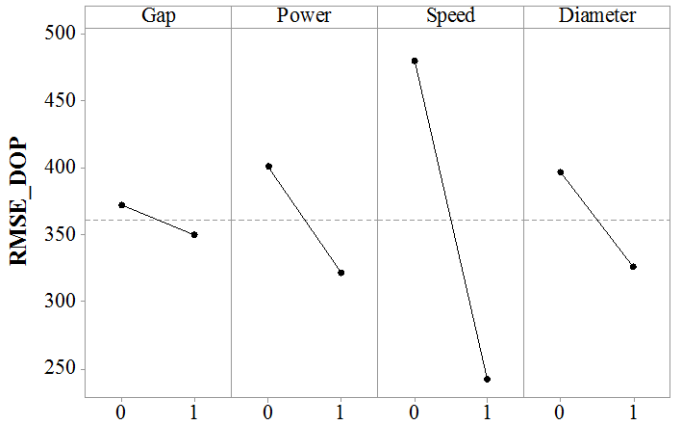

Figure 26 : Laser welding parameters effects on training MSE_DOP reduction

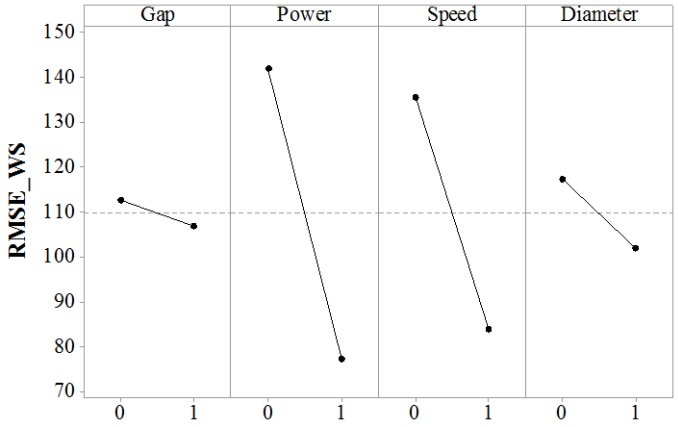

Figure 27 : Laser welding parameters effects on training MSE_WS reduction

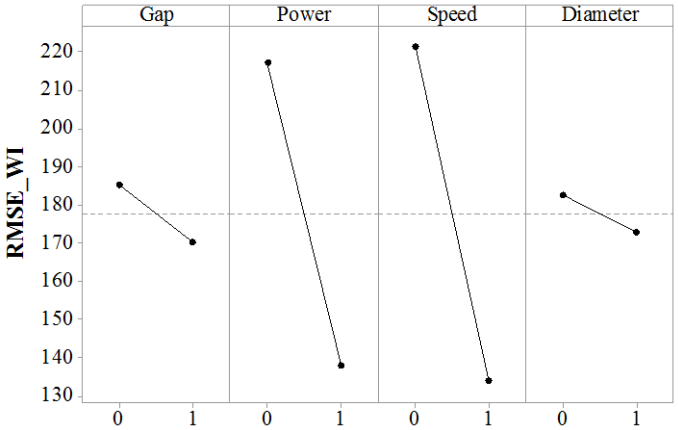

Figure 28 : Laser welding parameters effects on training MSE_WI reduction

The P-value and F-value express the reliability of ANOVA results. For example, for P = 0.03, the Gap contribution of 1.2% is a reliable result with 97% confidence. As we can see, the confidence interval for the effects of laser power, welding speed and focal diameter is about 99%, and that associated with the gap effect is 94%, this is most likely due to difficulty maintaining a constant Gap along the welding line.

A comparison between validation errors and learning errors shows how well an ANN model can predict the geometric attributes of the weld for any laser welding parameters combination. The comparison is applied to the models that show better performances during the learning process, namely models M_1, M_2, M_5 and M_8. **Table 17** includes learning errors, validation errors, and k-fold cross-validation error.

The results do not show a large deviation between training errors and validation errors, as the maximum gap between these two has been proved to not exceed 4%. The validation errors obtained by the two methods are almost identical. In the light of the results shown in the **Table 17**, the DOP can be predicted with a precision greater than 93% by the model M_1, a precision greater than 91% by the M_2 model and a prediction error exceeding 10% for the two other models. WS can be estimated with a precision greater than 95% by the four models. WI can be predicted by the model M_1 with an accuracy greater than 93% and a precision of 91% for other models. **Figure 29** shows the values predicted by the model M_1 Vs actual values, respectively of DOP, WS and WI. **Figure 30** shows those predicted by the model M_2 and **Figure 31** shows those predicted by model M_5. The contour of the cross section of a weld bead can be deduced from the three predicted geometric attributes DOP, WS and WI.

Table 15: Error estimates of training, hold-out set validation (Val_1) and 6-fold cross validation (Val_2) of the best models

Model	Limits	RMSE_DOP	MAPE_DOP	RMSE_WS	MAPE_WS	RMSE_WI	MAPE_WI
	Train	68.9	2.1	20.2	1.1	53.5	2.6
M1	Val1	134.01	6.05	48.51	3.1	133.4	6.81
	Val2	163.1	6.8	35.2	2.2	101.5	6.6
	Train	142.3	4.2	35.5	2.8	79.8	4.5
M2	Val1	194.6	8.2	62.4	4.2	166.4	8.7
	Val2	203.3	8.8	50.5	3.4	117.4	8.4
	Train	237.9	8.2	47.8	2.8	79.8	4.5
M5	Val1	330.2	12.9	68.7	4.2	152.3	7.6
	Val2	366.4	17.4	65.2	4.8	115.4	7.8
	Train	268.9	8.9	57.5	3.2	105.4	6.1
M8	Val1	337.2	13.6	80.5	4.9	168.4	8.7
	Val2	308.5	13.0	66.8	4.4	126.6	8.5

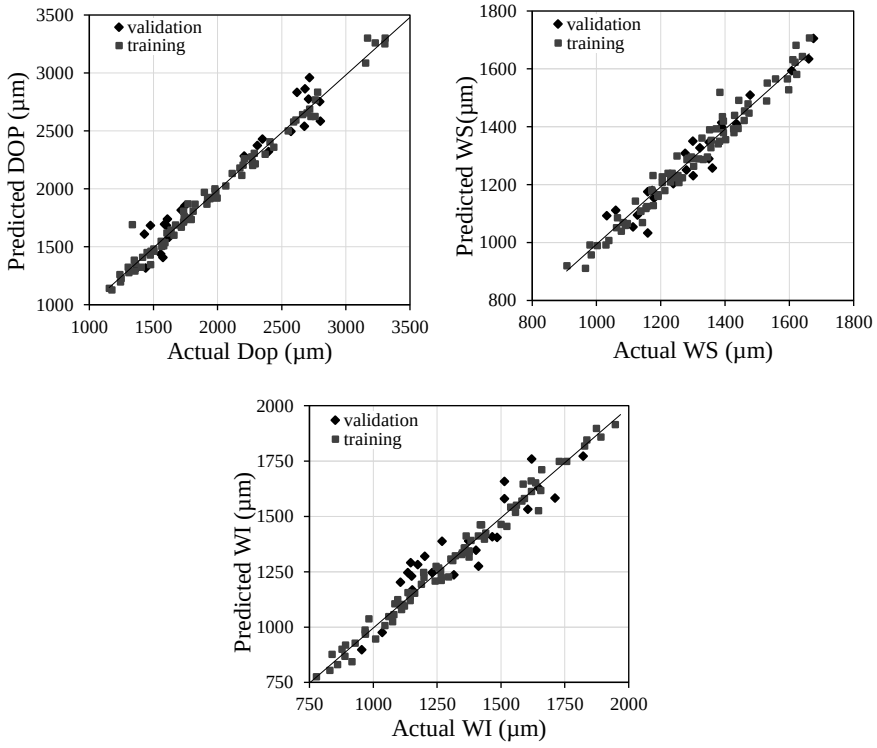

Figure 29 : Predicted Vs actual DOP, WS and WI using M1

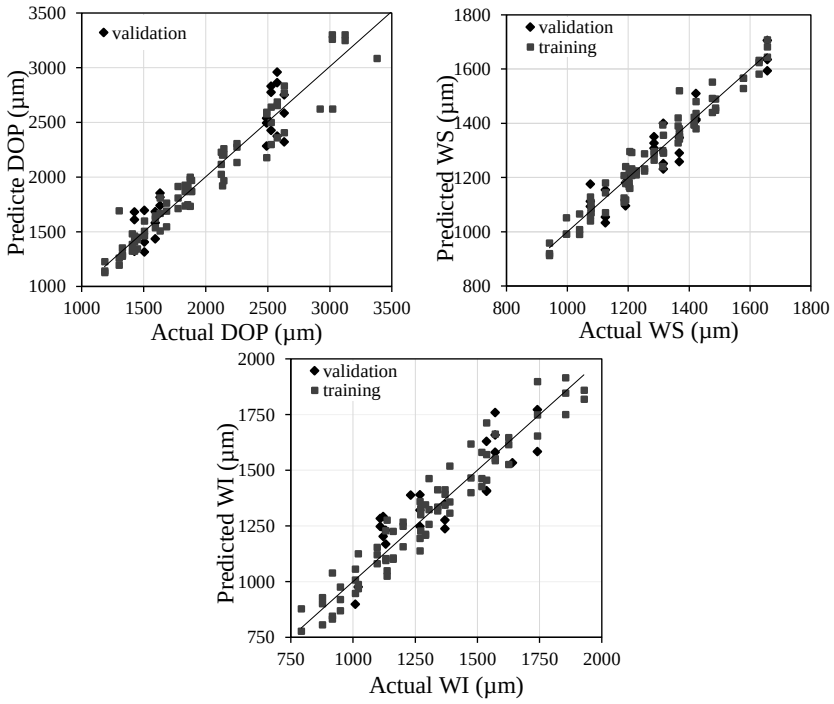

Figure 30 : Predicted Vs actual DOP, WS and WI using M2

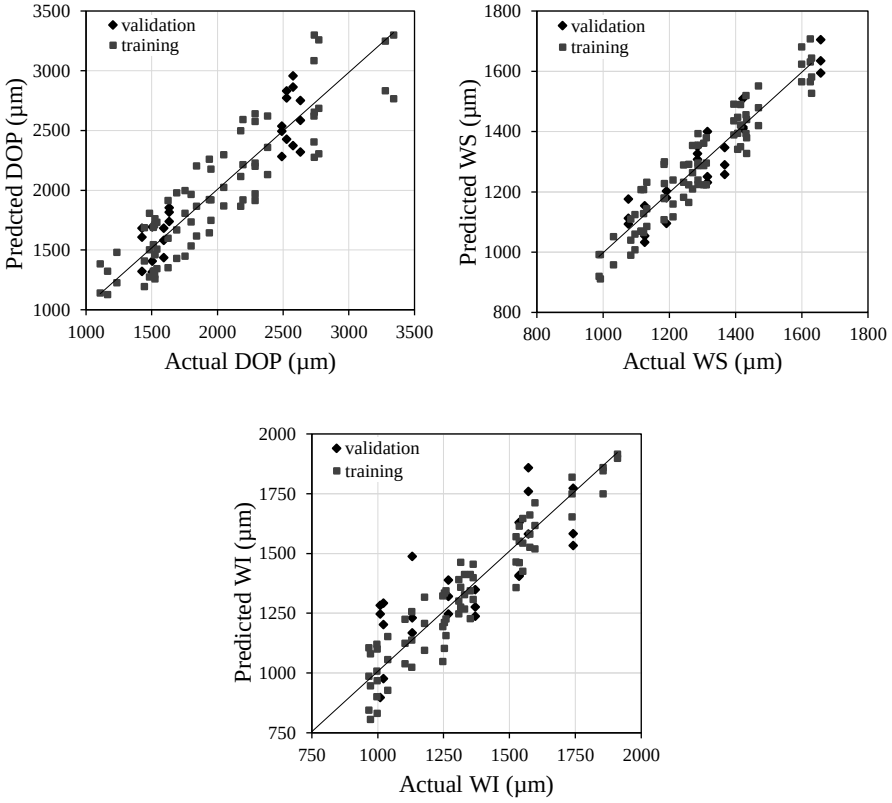

Figure 31 : Predicted Vs actual DOP, WS and WI using M5

3.6 CONCLUSION

This paper presents a structured approach developed to design an effective artificial neural network based model for predicting the weld bead dimensional characteristic in laser overlap welding of low carbon galvanized steel. Based on a fused data provided by structured experimental investigations using Taguchi method and in-depth FEM based 3D simulations, the possible relationships between welding parameters such as laser power, welding speed, laser beam diameter and gap, and weld bead dimensional characteristics such as depth of penetration, width at top surface and width at interface are analyzed and their sensitivity to the welding conditions are evaluated using relevant statistical tools. Based on these results, a factorial design is used to develop, implement and evaluate different neural network based

prediction models. The proposed models are trained and tested using experimental data, supported by the data generated by the 3D simulation. Hold-out test and k-fold cross validation combined to improved statistical criteria are used to evaluate the influence of the laser welding parameters on the performances of the models. Analyses of variance results reveal that all the welding parameters have a positive contribution to the improvement of the prediction quality. The laser power and the welding speed contributions are much more important compared to the contribution of the laser beam diameter. The gap contribution appears to be insignificant.

The achieved predictive modelling results demonstrate that the resulting models present excellent performances and can effectively predict the weld bead dimensional characteristics with average predicting errors less than 10%. The validation process reveals that the WS can be predicted with an accuracy of 96% while the prediction accuracy of DOP and WI is about 93%. These results demonstrate that the proposed ANN based prediction approach can effectively lead to a consistent model able to accurately and reliably provide an appropriate prediction of weld bead dimensional characteristics in laser overlap welding of low carbon galvanized steel under variable welding parameters and conditions.

With the encouraging results achieved using this modelling strategy, the laser overlap welding of low carbon galvanized steel will be the subject of additional and exhaustive investigations to produce more numerical simulation and experimental data as well as to test others neural networks approach in order to develop more efficient ANN predictive modelling method.

CONCLUSION GÉNÉRALE

Le présent projet de recherche porte sur le soudage au laser par recouvrement de l'acier galvanisé à faible teneur en carbone, largement utilisé pour la construction de la carrosserie automobile. Son objectif principal est l'exploitation efficace des avantages qu'offre ce procédé, pour obtenir des soudures sans défauts, ayant des caractéristiques qui répondent aux exigences de l'ingénierie automobile. Cela n'est possible que par un contrôle minutieux des paramètres du laser et des conditions de soudage. Afin de réaliser un tel objectif, une approche en trois étapes a été adoptée.

Dans un premier temps, une investigation expérimentale du procédé de soudage au laser par recouvrement de tôle en acier galvanisé a été conduite dans le but d'identifier les variables ayant un impact sur la qualité du joint de soudure, d'évaluer et d'analyser leurs effets et ceux de leurs interactions sur les caractéristiques géométriques de la soudure. Les relations de dépendance éventuelles entre ces variables et la qualité de la soudure ont également été investiguées. Les expérimentations ont été réalisées à l'aide d'un laser Nd-YAG 3KW suivant un plan d'expériences basé sur la méthode Taguchi. La puissance du laser, la vitesse de soudage, le diamètre du faisceau laser et le gap entre les tôles sont les paramètres qui ont été considérées comme variables dans cette investigation pour caractériser la variation d'attributs géométriques de la soudure tels que la profondeur de pénétration de la soudure (DOP), la largeur de la soudure à la surface (WS) et à l'interface (WI). L'analyse de la variance, les graphes d'effets, les pourcentages de contribution, le test de Fisher et la régression sont parmi les outils statistiques utilisés pour l'analyse des résultats expérimentaux. Globalement, les résultats montrent que les quatre paramètres ont des effets sur les trois caractéristiques géométriques de la soudure mais à des degrés variés. La profondeur de pénétration de la soudure est très sensible à la variation de la vitesse de soudage avec une contribution d'environ 67%. Les effets de la puissance et du diamètre du faisceau laser sont moins importants mais demeurent significatifs avec une contribution d'environ

15%. La vitesse et de la puissance sont les variables ayant les effets les plus prédominant sur la variation de la largeur de la soudure à la surface et à l'interface. Leurs contributions représentent environ 40% chacune. La contribution du diamètre focal dans la variation de WS et WI représente 15%. Malgré sa présence essentielle pour remédier aux problèmes liés au zinc, le gap a des effets négligeables. Ses contributions dans la variation des trois caractéristiques géométriques de la soudure représentent moins de 5%.

Les mesures de micro-dureté montrent des résultats cohérents avec une augmentation de la dureté de la soudure (250 Hv) par rapport à celle du métal de base (150Hv).

Dans un deuxième temps, une approche de modélisation numérique 3D par la méthode des éléments finis a été proposée pour simuler le comportement du procédé de soudage au laser dans des conditions difficiles à réaliser expérimentalement.

Le modèle numérique développé a été bâti en se basant sur les équations de transfert de chaleur en tenant compte des propriétés du matériau dépendant de la température et de l'enthalpie de changement de phase. Le modèle de source de chaleur utilisé a été adapté de manière à prendre en compte simultanément le soudage en mode conduction et en mode trou de serrure. Les résultats de la première phase ont été utilisés pour la validation expérimentale du modèle numérique 3D.

La comparaison des prédictions par rapport aux mesures expérimentales montre que le modèle présente des prédictions précises et cohérentes peu importe les paramètres et les conditions de soudage. La précision obtenue est supérieure à 95%. De plus, ce modèle a permis de réaliser une analyse exhaustive aussi bien qualitative que quantitative des effets et des contributions des paramètres de soudage sur la variation de la qualité de la soudure.

Cependant, malgré ses performances en termes de précision, le modèle numérique est peu adapté à une implémentation dans un processus de production. Étant très gourmand en temps de calcul, le temps nécessaire pour produire les prédictions est très long. Cependant, pour remédier à cette situation, un modèle prédictif utilisant les réseaux de neurones artificiels a été proposé pour permettre des prédictions rapides, précises et robustes. Le

développement de ce modèle fut l'objet de la troisième étape dans laquelle une large base de données combinant données expérimentales et données de simulation a servi à l'entrainement et à la validation de 16 versions du modèle neuronique. Chacun de ces modèles se base sur une combinaison spécifique de paramètres de soudage. Le meilleur modèle a été sélectionné parmi ces modèles en se basant sur plusieurs critères d'évaluation de la qualité des prédictions et de la capacité de généralisation de chaque modèle.

L'analyse des résultats du processus de modélisation montre que tous les paramètres et les conditions de soudage considérés contribuent positivement à l'amélioration de la qualité des prédictions. Les résultats montrent que le modèle obtenu permet des prédictions rapides et robustes compatibles avec les mesures expérimentales avec des erreurs de prédiction moyenne ne dépassant pas les 4% pour WS et 7% pour DOP et WI.

Bien que ces résultats soient très satisfaisants, des investigations numériques et expérimentales additionnelles sont souhaitables pour enrichir les données disponibles pour raffiner l'analyse des effets des différents paramètres sur la qualité du joint de soudure. Le problème de l'instabilité causée par l'évaporation prématurée du recouvrement du zinc à l'interface des tôles d'acier galvanisé devrait également retenir l'attention des chercheurs dans le domaine.

RÉFÉRENCES BIBLIOGRAPHIQUES

1. Maiman, T.H., *Stimulated optical radiation in ruby.* nature, 1960. **187**(4736): p. 493-494.
2. Handbook, A., *Volume 6: Welding, Brazing and Soldering.* ASM International, 1993. **2603**.
3. Miyamoto, I. and K. Mori. *Development of in-process monitoring system for laser welding*. in *International Congress on Applications of Lasers & Electro-Optics*. 1995. LIA.
4. Locke, E. and R. Hella, *Metal processing with a high-power CO 2 laser*. IEEE Journal of Quantum Electronics, 1974. **10**(2): p. 179-185.
5. Arata, Y. and I. Miyamoto, *Laser welding.* Technocrat, 1978. **11**(5): p. 33-42.
6. Duley, W., *CO2 lasers effects and applications*. 2012: Elsevier.
7. Leong, K., et al., *Threshold laser beam irradiances for melting and welding.* Journal of laser applications, 1997. **9**(5): p. 227-231.
8. Rai, R., et al., *Heat transfer and fluid flow during keyhole mode laser welding of tantalum, Ti–6Al–4V, 304L stainless steel and vanadium.* Journal of physics D: Applied physics, 2007. **40**(18): p. 5753.
9. Bäuerle, D., *Laser processing and chemistry*. 2013: Springer Science & Business Media.
10. Hann, D., J. Iammi, and J. Folkes, *A simple methodology for predicting laser-weld properties from material and laser parameters.* Journal of Physics D: Applied Physics, 2011. **44**(44): p. 445401.
11. Eagar, T. and N. Tsai, *Temperature fields produced by traveling distributed heat sources.* Welding journal, 1983. **62**(12): p. 346-355.
12. Ready, J.F., D.F. Farson, and T. Feeley, *LIA handbook of laser materials processing.* 2001.
13. Swift-Hook, D. and A. Gick, *Penetration welding with lasers.* Welding journal, 1973. **52**(11): p. 492s-499s.
14. Kong, F., et al., *Real-time monitoring of laser welding of galvanized high strength steel in lap joint configuration.* Optics & Laser Technology, 2012. **44**(7): p. 2186-2196.
15. Shaofeng, G., *The laser welding technology of three-layer zinc coated sheet.* WELDING AND JOINING-HARBIN-, 2006. **1**: p. 52.
16. Mei, L., et al., *Research on laser welding of high-strength galvanized automobile steel sheets.* Optics and Lasers in Engineering, 2009. **47**(11): p. 1117-1124.

17. Zhang, M., et al., *Observation of spatter formation mechanisms in high-power fiber laser welding of thick plate.* Applied Surface Science, 2013. **280**: p. 868-875.
18. Akhter, R., W. Steen, and K. Watkins, *Welding Zinc-Coated Steel with a Laser and the Properties of the Weldment.* Journal of Laser Applications, 1991. **3**(2): p. 9-20.
19. Li, X., W.S. Lawson, and Y.N. Zhou, *Lap welding of steel articles having a corrosion resisting metallic coating*. 2008, Google Patents.
20. Mazumder, J., A. Dasgupta, and M. Bembenek, *Alloy based laser welding*. 2002, Google Patents.
21. Gualini, M., S. Iqbal, and F. Grassi, *Modified dual-beam method for welding galvanized steel sheets in lap configuration.* Journal of Laser Applications, 2006. **18**(3): p. 185-191.
22. Yang, S. and R. Kovacevic, *Welding of galvanized dual-phase 980 steel in a gap-free lap joint configuration.* Welding Journal, 2009. **88**(8): p. 168-78.
23. Graham, M., et al., *Nd: YAG laser beam welding of coated steels using a modified lap joint geometry*. Welding Journal-Including Welding Research Supplement, 1996. **75**(5): p. 162s.
24. Fabbro, R., et al., *Study of CW Nd-Yag laser welding of Zn-coated steel sheets.* Journal of physics D: Applied physics, 2006. **39**(2): p. 401.
25. Pieters, R. and I. Richardson, *Laser welding of zinc coated steel in overlap configuration with zero gap.* Science and Technology of Welding and Joining, 2005. **10**(2): p. 142-144.
26. Benyounis, K. and A.-G. Olabi, *Optimization of different welding processes using statistical and numerical approaches–A reference guide.* Advances in engineering software, 2008. **39**(6): p. 483-496.
27. Huang, S.H. and H.-C. Zhang, *Artificial neural networks in manufacturing: concepts, applications, and perspectives.* IEEE Transactions on Components, Packaging, and Manufacturing Technology: Part A, 1994. **17**(2): p. 212-228.
28. Meireles, M.R., P.E. Almeida, and M.G. Simões, *A comprehensive review for industrial applicability of artificial neural networks.* IEEE transactions on industrial electronics, 2003. **50**(3): p. 585-601.
29. Balasubramanian, K., G. Buvanashekaran, and K. Sankaranarayanasamy, *Modeling of laser beam welding of stainless steel sheet butt joint using neural networks.* CIRP Journal of Manufacturing Science and Technology, 2010. **3**(1): p. 80-84.
30. Ribolla, A., G.L. Damoulis, and G.F. Batalha, *The use of Nd: YAG laser weld for large scale volume assembly of automotive body in white.* Journal of materials processing technology, 2005. **164**: p. 1120-1127.
31. Kim, J., S. Oh, and H. Ki, *A study of keyhole geometry in laser welding of zinc-coated and uncoated steels using a coaxial observation method.* Journal of Materials Processing Technology, 2015. **225**: p. 451-462.
32. Pieters, R., et al., *Zinc transport phenomena in laser welding of coated sheet steel in overlap configuration.* Welding in the World, 2008. **52**(7-8): p. 33-41.
33. Norman, P., I. Eriksson, and A. Kaplan, *Monitoring laser beam welding of zinc coated sheet metal to analyze the defects occurring*. 2009.

34. Norman, P., H. Engström, and A. Kaplan. *State-of-the-art of monitoring and imaging of laser welding defects*. in *11th NOLAMP Conference in Laser Processing of Materials*. 2007.
35. Chen, G., et al., *Research on key influence factors of laser overlap welding of automobile body galvanized steel.* Optics & Laser Technology, 2013. **45**: p. 726-733.
36. Bagger, C. and F.O. Olsen, *Review of laser hybrid welding.* Journal of laser applications, 2005. **17**(1): p. 2-14.
37. Dasgupta, A. and J. Mazumder. *A novel method for lap welding of automotive sheet steel using high power CW CO2 laser*. in *Proceedings of the 4th International Congress on Laser Advanced Materials Processing*. 2006.
38. Sinha, A.K., D.Y. Kim, and D. Ceglarek, *Correlation analysis of the variation of weld seam and tensile strength in laser welding of galvanized steel.* Optics and Lasers in Engineering, 2013. **51**(10): p. 1143-1152.
39. Zhao, Y., et al., *Optimization of laser welding thin-gage galvanized steel via response surface methodology.* Optics and Lasers in Engineering, 2012. **50**(9): p. 1267-1273.
40. Wei, S., et al., *Effects of welding parameters on fibre laser lap weldability of galvanised DP1000 steel.* Science and Technology of Welding and Joining, 2015. **20**(5): p. 433-442.
41. Schmidt, M., A. Otto, and C. Kägeler, *Analysis of YAG laser lap-welding of zinc coated steel sheets.* CIRP annals, 2008. **57**(1): p. 213-216.
42. Dagli, C.H., *Artificial neural networks for intelligent manufacturing*. 2012: Springer Science & Business Media.
43. Kazemi, K. and J.A. Goldak, *Numerical simulation of laser full penetration welding.* Computational Materials Science, 2009. **44**(3): p. 841-849.
44. Wang, J., et al., *Development of a new combined heat source model for welding based on a polynomial curve fit of the experimental fusion line.* The International Journal of Advanced Manufacturing Technology, 2016. **87**(5-8): p. 1985-1997.
45. Chande, T. and J. Mazumder, *Estimating effects of processing conditions and variable properties upon pool shape, cooling rates, and absorption coefficient in laser welding.* Journal of applied physics, 1984. **56**(7): p. 1981-1986.
46. Courtois, M., et al. *Keyhole formation during spot laser welding: Heat and fluid flow modeling in a 2D axisymmetric configuration*. in *COMSOL Conference, Milan*. 2012.
47. Bruyere, V., C. Touvrey, and P. Namy. *A phase field approach to model laser power control in spot laser welding*. in *Proceedings of the 2014 Comsol Conference Cambridge*. 2014.
48. Steen, W.M. and J. Mazumder, *Laser material processing*. 2010: springer science & business media.
49. Rosenthal, D., *The theory of moving sources of heat and its application of metal treatments.* Transactions of ASME, 1946. **68**: p. 849-866.
50. Friedman, E., *Thermomechanical analysis of the welding process using the finite element method.* 1975.
51. Ashby, M. and K.E. Easterling, *The transformation hardening of steel surfaces by laser beams—I. Hypo-eutectoid steels.* Acta metallurgica, 1984. **32**(11): p. 1935-1948.

52. Goldak, J., A. Chakravarti, and M. Bibby, *A new finite element model for welding heat sources.* Metallurgical transactions B, 1984. **15**(2): p. 299-305.
53. Cline, H. and T. Anthony, *Heat treating and melting material with a scanning laser or electron beam.* Journal of Applied Physics, 1977. **48**(9): p. 3895-3900.
54. Davis, M., et al., *Heat hardening of metal surfaces with a scanning laser beam.* Journal of Physics D: Applied Physics, 1986. **19**(10): p. 1981.
55. Bradley, J.R., *A simplified correlation between laser processing parameters and hardened depth in steels.* Journal of Physics D: Applied Physics, 1988. **21**(5): p. 834.
56. Mackwood, A. and R. Crafer, *Thermal modelling of laser welding and related processes: a literature review.* Optics & Laser Technology, 2005. **37**(2): p. 99-115.
57. Chukkan, J.R., et al., *Simulation of laser butt welding of AISI 316L stainless steel sheet using various heat sources and experimental validation.* Journal of Materials Processing Technology, 2015. **219**: p. 48-59.
58. Semak, V.V., B. Damkroger, and S. Kempka, *Temporal evolution of the temperature field in the beam interaction zone during laser material processing.* Journal of Physics D: Applied Physics, 1999. **32**(15): p. 1819.
59. Chan, C., J. Mazumder, and M. Chen, *A two-dimensional transient model for convection in laser melted pool.* Metallurgical Transactions A, 1984. **15**(12): p. 2175-2184.
60. Bannour, S., et al., *Effects of temperature-dependent material properties and shielding gas on molten pool formation during continuous laser welding of AZ91 magnesium alloy.* Optics & Laser Technology, 2012. **44**(8): p. 2459-2468.
61. Kannatey-Asibu Jr, E., *Principles of laser materials processing*. Vol. 4. 2009: John Wiley & Sons.
62. Oussaid, K., A. El Ouafi, and A. Chebak, *Experimental Investigation of Laser Welding Process in Overlap Joint Configuration.* Journal of Materials Science and Chemical Engineering, 2019. **7**(3): p. 16-31.
63. Sathiya, P., K. Panneerselvam, and M.A. Jaleel, *Optimization of laser welding process parameters for super austenitic stainless steel using artificial neural networks and genetic algorithm.* Materials & Design (1980-2015), 2012. **36**: p. 490-498.
64. Zhang, G., B.E. Patuwo, and M.Y. Hu, *Forecasting with artificial neural networks:: The state of the art.* International journal of forecasting, 1998. **14**(1): p. 35-62.
65. Campbell, S., A. Galloway, and N. McPherson, *Artificial neural network prediction of weld geometry performed using GMAW with alternating shielding gases.* Welding Journal, 2012. **91**(6): p. 174S-181S.
66. Farson, D., K. Fang, and J. Kern. *Intelligent laser welding control*. in *International Congress on Applications of Lasers & Electro-Optics*. 1991. LIA.
67. Luo, H., et al., *Application of artificial neural network in laser welding defect diagnosis.* Journal of Materials Processing Technology, 2005. **170**(1-2): p. 403-411.
68. Chandrasekhar, N., et al., *Intelligent modeling for estimating weld bead width and depth of penetration from infra-red thermal images of the weld pool.* Journal of Intelligent Manufacturing, 2015. **26**(1): p. 59-71.

69. Acherjee, B., et al., *Application of artificial neural network for predicting weld quality in laser transmission welding of thermoplastics.* Applied soft computing, 2011. **11**(2): p. 2548-2555.
70. Olabi, A., et al., *An ANN and Taguchi algorithms integrated approach to the optimization of CO2 laser welding.* Advances in Engineering Software, 2006. **37**(10): p. 643-648.
71. Casalino, G. and F.M.C. Minutolo, *A model for evaluation of laser welding efficiency and quality using an artificial neural network and fuzzy logic.* Proceedings of the Institution of Mechanical Engineers, Part B: Journal of Engineering Manufacture, 2004. **218**(6): p. 641-646.
72. Paliwal, M. and U.A. Kumar, *Neural networks and statistical techniques: A review of applications.* Expert systems with applications, 2009. **36**(1): p. 2-17.
73. Jacques, L. and A. El Ouafi, *ANN Based Predictive Modelling of Weld Shape and Dimensions in Laser Welding of Galvanized Steel in Butt Joint Configurations.* Journal of Minerals and Materials Characterization and Engineering, 2018. **6**(03): p. 316.
74. Oussaid, K. and A. El Ouafi, *A Three-Dimensional Numerical Model for Predicting the Weld Bead Geometry Characteristics in Laser Overlap Welding of Low Carbon Galvanized Steel.* Journal of Applied Mathematics and Physics, 2019. **7**(10): p. 2169.